Inter-comparison Review of IPWV retrieved from INSAT-3DR Sounder, GNSS & CAMS Reanalysis Data

Ramashray Yadav, Ram Kumar Giri and Virendra Singh

Satellite Meteorology Division, India Meteorological Department, Ministry of Earth Sciences

New Delhi-110003

Abstract:

The spatiotemporal variations of integrated precipitable water vapor (IPWV) are very important to understand the regional variability of water vapour. Traditional in-situ measurements of IPWV in Indian region are limited and therefore the performance of satellite and Copernicus Atmosphere Meteorological Service (CAMS) retrieval with Indian Global Navigation Satellite System (GNSS) taking as reference has been analyzed. In this study the CAMS reanalysis data one year (2018), Indian GNSS and INSAT-3DR sounder retrievals data for one & half years (January-2017 to June-2018) has been utilized and computed statistics. It is noticed that seasonal correlation coefficient (CC) values between INSAT-3DR and Indian GNSS data mainly lie within the range of 0.50 to 0.98 for all the selected 19 stations except Thiruvanathpuram (0.1), Kanyakumari (0.31), Karaikal (0.15) during monsoon and Panjim (0.2) during post monsoon season respectively. The seasonal CC values between CAMS and INSAT-3DR IPWV are ranges 0.73 to .99 except Jaipur (0.16) & Bhubneshwar (0.29) during pre-monsoon season, Panjim (0.38) during monsoon, Nagpur (0.50) during post-monsoon and Dibrugarh (0.49) Jaipur (0.58) & Bhubaneswar (0.16) during winter season respectively .The root mean square error (RMSE) values are higher under the wet conditions (Pre Monsoon & Monsoon season) than under dry conditions (Post Monsoon & Winter season) and found differences in magnitude and sign of bias of INSAT-3DR, CAMS with respect to GNSS IPWV from station to station and season to season.

This study will help to improve understanding and utilization of CAMS and INSAT-3DR data more effectively along with GNSS data over land, coastal and desert locations in terms of seasonal flow of IPWV which is an essential integrated variable in forecasting applications.

Keywords: Indian Satellite -3DR (INSAT-3DR), Integrated Precipitable Water Vapour (IPWV), Copernicus Atmospheric Monitoring Service (CAMS) & Global Navigation Satellite System (GNSS).

Introduction

Integrated precipitable water vapor (IPWV) is a meteorological factor that shows the amount of water vapour contained in the column of air per unit area of the atmosphere in terms of the depth of liquid (Viswanadham et al., 1981). This parameter has great importance in all studies related to the atmosphere and its properties throughout the year and in all seasons. The assessment of IPWV is done in many ways as in situ, model based or through remote sensing measurements. The in situ measurements have limited coverage, expensive and require maintenance of all the time. Remote sensing instruments, especially absorption in the infrared and microwave region of the solar spectrum have wide coverage, cheaper, almost maintenance free but needs to validate their retrieval performance and inter comparison before applying in the operational meteorological service domain. Similarly, model based data have limitations to capture the localized features of convection due to sparseness or very few numbers of the quality controlled observational data over that region. Water vapour content present in the atmosphere, one of the most influential constituents of the atmosphere, is responsible for determining the amount of precipitation that a region can receive (Trenberth et al., 2003). The absorptions of surface radiation depends on wavelength and water vapor content. Each absorbing water vapour molecule emits radiation according to Planck's law, mainly depending on its temperature and the extent of absorption differs depending on the wavelength, the satellite sees different levels of atmosphere.

In Global Ozone Monitoring Experiment (GOME) and Scanning Imaging Absorption Spectrometer for Atmospheric CHartography (SCIAMACHY), both used the principle of differential optical absorption spectroscopy in red spectral range of IPWV retrieval (Beirle et al, 2018). Atmospheric Infrared sounder is a hyper spectral instrument which collects radiances in 2378 IR channels with wavelength ranging from 3.7 to 15.4 µm. Cloud cleared radiances of AIRS were utilized in the retrieval of column integrated water vapour which is contributed by a number of channels having different sensitivity towards water vapour content present in the atmosphere. (Aumann et al., 2003). Moderate Resolution Imaging Spectroradiometer (MODIS) utilized infrared algorithm employs ratios of water vapor absorbing channels at 0.905 µm, 0.936 µm, and 0.940 µm with atmospheric window channels at 0.865 µm and 1.24 µm estimated the precipitable water vapour (Kaufman and Gao, 1992).

The uncertainties in the retrieval of precipitable water vapor from satellites (like errors of calibration of channels, viewing geometry, radiative transfer in the forward models) are already addressed by previous studies (Ichoku et al., 2005 for MODIS, Noel et al., 2008 for GOME-2 and SCIAMACHY, Susskind et al., 2003, 2006 for AIRS). Wagner et al., 2006 studied GOME data for the period of 1996-2002 and reported globally and yearly averaged 2.8 ±0.8% increase of total column precipitable water (excluding the ENSO period).

The retrievals from reanalysis data sets Modern-Era Retrospective analysis for Research and applications-2 (MERRA-2) Gelaro et al., 2017 , Climate Forecast System Reanalysis (CFSR) (Saha et al., 2010) Data Archive at https://rda.ucar.edu/pub/cfsr.html utilized 3d-var data assimilation techniques and well captured the interannual variations of precipitable water vapour in the south of the Central Asia (Jiang et al., 2019). The study carried out by Berrisford et al., 2011, found ERA interim data set is superior in quality than ERA 40 during the period 1989-2008.

Ramashray et al., 2020 carried out the validation of Indian GNSS IPWV with GPS Sonde data for the period of June 2017 to May 2018 over Indian region and found reasonably well in agreement with in situ observations. In situ Radiosonde observations generally suffer spatiotemporal inhomogeneity errors and differences in relative humidity measured by different sensors. In this study he brought out positive bias less than 4.0 mm for 7 stations, correlation coefficient greater than 0.85 and RMSE less than 5.0 mm for all 09 collocated GPS sonde stations. In this direction the work carried out by Turner et al., 2003, 5 % dry bias with Microwave Radiometer and Vaisala RS80-H will be very useful while dealing with such Radiosonde observations. Miloshevich et al., 2009, found a similar limitation of Relative Humidity measurement with Vaisala RS92 Radio sonde and derived an empirical correction to remove the mean bias error, yielding bias uncertainty is independent of height.

The study carried out by Falaiye et al., 2018 is very important for considering the conventional data from long term observing stations of Indian domain along with the available model to establish the similar empirical relationship of getting the precipitable water vapour. This will also support to generate improved climatological mean especially over the remote regions.

Geo satellites have higher temporal resolution and continuous coverage and are important for monitoring the extreme weather events. Polar satellites have higher advantage higher spatial resolution and can operate both cloudy and non-cloudy conditions more effectively as compared to Geo satellites. Courcoux and Schroder et al., 2013, worked out the accuracies of Satellite Application Facility on Climate Monitoring (CMSAF) satellite Advanced Television and Infrared Observation Satellite Operational Vertical Sounder (ATOVS) precipitable water vapour of about 2-4 mm with respect to radiosonde and Atmospheric Infrared Sounder (AIRS) data both over land and ocean with resolution of 0.5º x 0.5º.

Geo-stationary Earth Orbit (GEO) satellites can produce data more timely and frequently. The retrieved high temporal resolution, Integrated Precipitable Water vapour (IPWV) from GEO satellites sensor data can be utilized to monitor pre-convective environments and predict heavy rainfall, convective storms, and clouds that may cause serious damage to human life and infrastructure (Martinez et al., 2007; Liu et al., 2019; Lee et al., 2015). At present two advanced Indian geostationary meteorological satellites INSAT-3D (launched on 26 July, 2013) and INSAT-3DR on 6 September, 2016) with similar sensor characteristics are orbiting over Indian Ocean region and are placed at 82° E and 74° E respectively. INSAT -3D & INSAT-3DR both satellites are equipped with the infrared sounders with 19 channels, which are used to provide meteorological parameters like the profiles of temperature, humidity and ozone, atmospheric stability indices, atmospheric water vapor, etc. at 1 hour (sector A) and 1.5 hour (sector B) intervals (Kishtawal et al., 2019). Temperature and humidity (T-q profile) is used to retrieve thermodynamic indices which is useful in analyzing the strength and severity of severe weather events. Therefore, IPWV is one of the critical variables used by forecasters when severe weather conditions are expected (Lee et al., 2016). Copernicus Atmosphere Monitoring Service (CAMS) global reanalysis (EAC4) latest data set of atmospheric composition has been built at approximate 80 km resolution with improved biases and consistent with time. (Inness et al., 2019).The concept of GNSS meteorology was first introduced by Bevis et al.,1992, 1994 and Businger et al., 1992 and IPWV data were estimated from Global Navigation Satellite System (GNSS) observations. In this study we have taken 19 Indian GNSS stations (10 inland, 8 coastal and 1 desert) or sites for study. Earlier studies (Jade et al., 2005; Jade and Vijayan et al., 2008; Puviarasan et al., 2014) of water vapour over the Indian subcontinent and surrounding ocean have shown strong seasonal variations.

The behavior of coastal regions are generally different from inland and desert stations as coastal regions greatly influenced moisture advection from breezing of the seas, which is the cause of the continuous increment of IPWV even after the air temperature decreased (Ortiz de Galisteo et al., 2011).

Perez-Ramirez et al., 2014, compared Aerosol Robotic Network (AERONET) precipitable water vapour retrievals from Sun photometers with radiosonde, ground based Microwave radiometry, GPS and found a consistent dry bias approximately 5-6 % with total uncertainties of 12-15 % in the retrievals of precipitable water vapour from AERONET. The study Perez-Ramirez et al., (2019) clearly brought out the importance of Maritime Aerosol. Network (MAN) in retrieving the precipitable water vapour over remote oceanic areas. The reanalysis model estimates have very good agreement with MAN with mean differences of ~ 5 % and standard deviation of ~15 % under clear sky conditions. The work done in the past by Smirnov et al., 2004, 2011, in retrieving the precipitable water vapour from aerosol network data especially for marine areas is very helpful to carry out further studies in future with INSAT-3DR satellite observations over oceanic areas.

The present study have two fold objectives (1) Inter-comparison of CAMS and INSAT-3DR, IPW retrievals with Indian GNSS stations by taking GNSS reference and (II) performance in the retrievals CAMS and INSAT-3DR sounder for both land and ocean regions. This analysis will be very useful to know about the satellite and reanalysis uncertainties and their improvements over place to place and season to season. It will also further improve and help the forecasters to use models as well as INSAT-3DR data sets with confidence as these are available over wide spatial coverage as compared to low density of GNSS network data over Indian domains.

2. Methodology and Data collection

The measured Integrated Precipitable Water Vapour (IPWV) from the India Meteorological Department (IMD) GNSS network with 15 minute temporal resolution data are used for the comparison of INSAT-3DR geostationary satellite IPWV products and CAMS reanalysis IPWV data. The INSAT-3DR data scans are each of one hour intervals from January-2017 to June-2018.

These measured and derived IPWV products are arranged as co-location of both temporal and spatial. The spatial views of the observational locations of GNSS and along with INSAT-3DR IPWV annual mean values are shown in Figure 2. The number of observational points (N) of each GNSS, INSAT-3DR and CAMS reanalysis of each station with its latitude, longitude are shown in Table 2. Here, winter season is considered as December, January and February months; pre monsoon season is considered as March, April and May; monsoon season in June, July and August months; finally post monsoon season is considered as September, October and November months.

2.1 IMD IPWV observation network

The ground based GNSS IPWV estimated at a high temporal sampling (15 minute) data (January 2017- June 2018) of Indian GNSS network is processed at satellite division of India Meteorological Department, Lodi Road, New Delhi. The data is processed daily by using the Trimble Pivot Platform (TPP) software.

The data is used operationally and archive as daily, weekly, monthly as well as seasonal basis for future utilization and dissemination to the users, researchers as per the official norms. If we reduce the cut off angle from 5º multipath effect will occur and introduce inaccuracy in the IPWV estimation. An elevation angle of greater than 5° is set for all stations to avoid the satellite geometry change and multipath effects. This is an optimum setting as a higher cut off angle (> 5°) may introduce dry bias in the IPWV estimation and notable 0.8 mm error in IPWV (Emardson et al., 1998). The other possible sources of error associated with GNSS data are mean temperature of atmosphere, dynamical pressure and isotropic errors. These errors will vary with location and time of observations.

2.2 Integrated Precipitable Water Vapour retrievals from INSAT-3DR Sounder data

The Sounder payload of the INSAT-3DR satellite has the capability to provide vertical profiles of temperature (40 levels from surface to ~ 70 km) and humidity (21 levels from surface to ~ 15 km) from surface to top of the atmosphere. The Sounder has eighteen narrow spectral channels in shortwave infrared, middle infrared and long wave infrared regions and one channel in the visible region. The ground resolution at nadir is 10 × 10 km for all nineteen channels. Specifications of sounder channels are given in Table 1. Vertical profiles of temperature and moisture can be derived from radiances in these 18 IR channels, using the first guess from numerical weather prediction (NWP) model data. INSAT-3DR sounder channels brightness temperature values are averaged over a number of fields of view (FOVs) prior to application of retrieval algorithm. Based on this, average vertical profiles are retrieved at 30 x 30 km (3 × 3 pixels) for each cloud free pixel.

As INSAT-3DR IPWV is sensitive to the presence of clouds in the field of view (limitation of Infra-red sounder sensors), hence the IPWV values collected under clear sky conditions were used in this study. Atmospheric profile retrieval algorithm for INSAT-3DR Sounder is a two-step approach. The first step includes generation of accurate hybrid first guess profiles using a combination of statistical regression retrieved profiles and model forecast profiles. The second step is nonlinear physical retrieval to improve the resulting first guess profile using Newtonian iterative method. The retrievals are performed using clear sky radiances measured by sounder within a 3x3 field of view (approximately 30x30 km resolution) over land for both day and night (similar to INSAT-3D ATBD, 2015). Four sets of regression coefficients are generated, two sets for land and ocean daytime conditions and the other two sets for land and ocean night-time conditions using a training dataset comprising historical radiosonde observations representing atmospheric conditions over INSAT-3DR observation region. Integrated Precipitable Water Vapour in mm can be given as:

$$PWV = \int_{p_1}^{p_2} \frac{q}{g\rho_w} dp$$

Where, 'g' is the acceleration of gravity, p_1 = surface pressure, p_2 = top of atmosphere pressure (i.e. about 100 hPa beyond which water vapour amount is assumed to be negligible). Unit of precipitable water is mm depth of equal amount of liquid water above a surface of one square meter. IMD is computing IPWV from 19 channel sounder of INSAT-3DR in three layers i.e. 1000-900 hPa, 900-700 hPa, 700-300 hPa and total PWV in the vertical column of atmosphere stretching from surface to about 100 hPa during cloud free condition. Monsoon, severe weather, cloudy condition puts the limitation for sounder profile (Venkat Ratnam et al., 2016). The GNSS and INSAT-3DR retrieved IPWV values are matched at every hour.

2.3 Scan Strategy of INSAT-3DR Sounder

The Sounder measures radiance in eighteen infrared (IR) and one visible channel simultaneously over an area of area of 10 km x 10 km at nadir every 100 ms. Using a two-axes gimballed scan mirror, this footprint can be positioned anywhere in the field of regard (FOR)- 24º (E-W) x 19º (N-S). To Sound the entire globe area of 6400 km x 6400 km in size, it takes almost three hours. A scan program mode allows sequential sounding of a selected area with periodic space and calibration looks. In this mode, a 'frame' consisting of multiple 'blocks' of the size 640 km x 640 km, can be sounded. The selected frame can be placed anywhere within a 24º (E-W) x 19º (N-S) (similar to INSAT-3D ATBD, 2015). An optimized scan strategy of sounder payload is worked out involving all stakeholders in such a way Indian land region sector-A data covered up on hourly basis and Indian Ocean region Sector-B data covered up on one & half hourly basis as shown in Figure 1. The full aperture internal Black-body calibration is performed every 30 min or on command based whenever required. The sounder payload has a provision to be carried out on board IR calibration, in which the scan mirror pointed towards the space look to measure the radiances then pointed to the internal blackbody present on the payload for measuring its radiances. There is also a provision to measure the temperature of the internal black body. All these data sets are transmitted along with video data of payload. During the processing at ground, the data collected during on board calibration are used to generate the calibration look up table for each scan. This enables the derivation of vertical profiles of temperature and humidity more accurately. These vertical profiles can then be used to derive various atmospheric stability indices and other parameters such as atmospheric water vapor content and total column ozone amount. The products derived over sector-A data are used for weather forecasting on operational basis and products derived over sector-B are used for assimilation in NWP model.

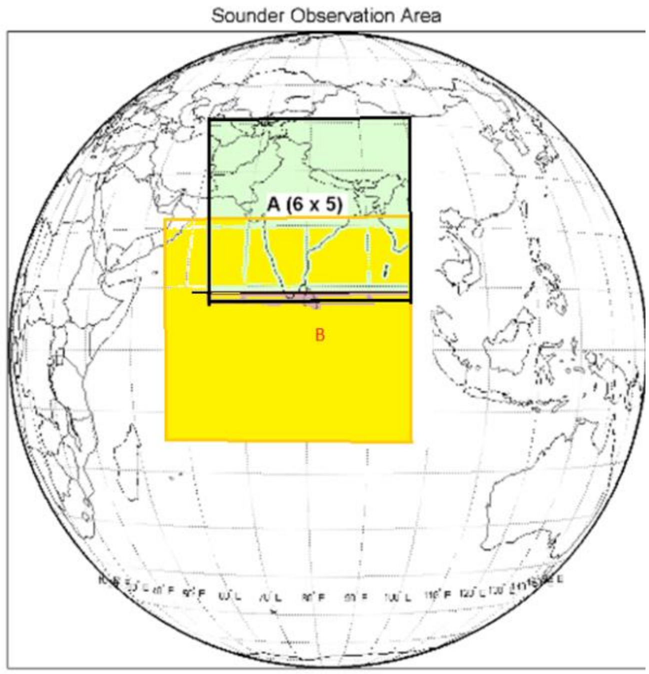

Sector-A Sector-B

0300, 0400, 0500 UTC-INSAT-3DR 0000, 0130 UTC INSAT-3DR

Figure 1.Scan Strategy and Area of Coverage of INSAT-3DR Sounder payload.

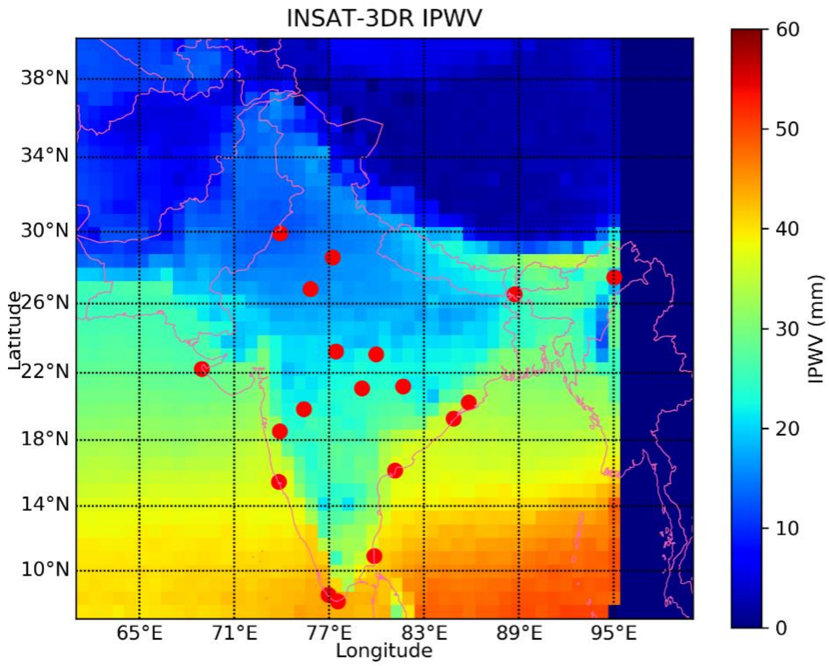

Figure 2. The annual mean of IPWV over India retrieved from INSAT- 3DR during the year of 2018.The geographical distribution of 19 GNSS stations (filled Red color circles).

Table 1. INSAT-3DR Sounder channel specifications

INSAT-3DR Sounder Channels Characteristics				
Detector	Channel No.	Central Wavelength (μm)	Principal absorbing gas	Purpose
Long wave	1	14.67	CO_2	Stratosphere temperature
	2	14.32	CO_2	Tropopause temperature
	3	14.04	CO_2	Upper-level temperature
	4	13.64	CO_2	Mid-level temperature
	5	13.32	CO_2	Low-level temperature
	6	12.62	water vapor	Total precipitable water
	7	11.99	water vapor	Surface temp., moisture
Mid wave	8	11.04	Window	Surface temperature
	9	9.72	Ozone	Total ozone
	10	7.44	water vapor	Low-level moisture

	11	7.03	water vapor	Mid-level moisture
	12	6.53	water vapor	Upper-level moisture
Short wave	13	4.58	N_2O	Low-level temperature
	14	4.53	N_2O	Mid-level temperature
	15	4.46	CO_2	Upper-level temperature
	16	4.13	CO_2	Boundary-level temp.
	17	3.98	Window	Surface temperature
	18	3.76	Window	Surface temp., moisture
Visible	19	0.695	Visible	Cloud

Table 2. List of GNSS stations (latitude, longitude, height) and location environment

S.No	Station	Station code	Long	Lat	Ellipsoid Height(m)	Environment
1	Aurangbad	ARGD	75.39	19.87	528.13	Inland
2	Bhopal	BHPL	77.42	23.24	476.22	Inland
3	Dibrugarh	DBGH	95.02	27.48	55.76	Inland
4	Delhi	DELH	77.22	28.59	165.06	Inland
5	Jabalpur	JBPR	79.98	23.09	355.09	Inland
6	Jaipur	JIPR	75.81	26.82	335.37	Inland
7	Jalpaiguri	JPGI	88.71	26.54	37.41	Inland
8	Pune	PUNE	73.88	18.53	487.72	Inland
9	Raipur	RIPR	81.66	21.21	245.56	Inland
10	Nagpur	NGPR	79.06	21.09	253.57	Inland
11	Dwarka	DWRK	68.95	22.24	-40.12	Costal
12	Gopalpur	GOPR	84.87	19.3	-15.94	Costal
13	Karaikal	KRKL	79.84	10.91	-79.07	Costal
14	Kanyakumari	KYKM	77.54	8.08	-49.23	Costal
15	Machilipattnam	MPTM	81.15	16.18	-61.07	Costal
16	Panjim	PNJM	73.82	15.49	-23.04	Costal
17	Thiruvanathpuram	TRVM	76.95	8.5	-18.44	Costal
18	Bhubneshwar	BWNR	85.82	20.25	-16.72	Costal
19	Sriganganagar	SGGN	73.89	29.92	132.17	Desert

2.4 Copernicus Atmosphere Monitoring Service (CAMS) reanalysis data

The CAMS reanalysis was produced using 4DVar data assimilation in European Centre for Medium Range Weather Forecasts (ECMWF) Integrated Forecasting System (IFS), with 60 hybrid sigma / pressure (model) levels in the vertical, with the top level at 0.1 hPa (https://ads.atmosphere.copernicus.eu/cdsapp#!/search?type=dataset). Atmospheric data are available on these levels and they are also interpolated to 25 pressure levels, 10 potential temperature levels and 1 potential vorticity level (Inness et al., 2019).This new reanalysis data set has horizontal resolution of about 80 km (0.75° x 0.75°), smaller biases for reactive gases and aerosols, improved and more consistent with time as compared to earlier versions. INSAT-3DR Data set has horizontal resolution at 30 x 30 km (3 × 3 pixels) for each cloud free pixel. Collocation match up has been created at 0.75° x 0.75° (about 80 km) spatial resolution for comparison and performance of INSAT-3DR data with CAMS reanalysis data using bilinear interpolation technique. Temporal domains are selected at 00, 03, 06, 09, 12, 15, 18, 21 UTC time interval for Indian GNSS along with INSAT-3DR at 03, 09, 15, 21 UTC for performance analysis. The CAMS reanalysis IPWV retrievals are interpolated to different geographical locations of 19 GNSS observations. We have used nearest neighbor interpolation techniques to interpolate CAMS reanalysis with GNSS data. In this method we evaluate each station to determine the number of neighboring grid cells in 0.75° x 0.75° box that surround the GNSS station and contain at least one valid CAMS reanalysis data. CAMS data is capable of capturing large scale features of moisture flow which help the forecasters in predicting large scale weather systems such as western disturbances, cyclonic storms, monitoring of monsoon and other associated weather events affecting throughout the year in Indian domain.

2.5 Analysis of statistical skill scores

The collocated comparison statistics with matchup data set is used to evaluate the statistical performance of retrievals of INSAT-3DR and CAMS with respect to GNSS IPWV over Indian region.

The statistical metrics used for quantitative evaluation are, linear correlation coefficient (CC), Standard Deviation (SD), Bias and Root Mean Square Error (RMSE).The computation of above said statistical metrics are given below:

Let, O_i represents the i^{th} observed value of INSAT-3DR or CAMS reanalysis data and M_i represents the i^{th} GNSS IPWV value for a total of n observations.

Mean bias (MB)

$$\mathrm{MB} = \frac{1}{\mathrm{n}} \sum_{i=1}^{N} (\mathrm{O_i} - M_i)$$

Root Mean Squared Error (RMSE)

$$RMSE = \sqrt{\frac{1}{N}\sum_{i=1}^{N}(O_i - M_i)^2}$$

Correlation Coefficient (CC)

$$CC = \frac{N(\sum_{i=1}^{N} M_i O_i) - (\sum_{i=1}^{N} M_i)(\sum_{i=1}^{N} O_i)}{\sqrt{[N\sum_{i=1}^{N} M^2{}_i - (\sum_{i=1}^{N} M_i)^2][N\sum_{i=1}^{N} O^2{}_i - (\sum_{i=1}^{N} O_i)^2]}}$$

Standard Deviation (SD)

$$\mathrm{SD} = \sqrt{\left\{\frac{[N\sum_{i=1}^{N}(M_i - \overline{M})^2][N\sum_{i=1}^{N}(O_i - \overline{O})^2]}{N}\right\}}$$

2.6 INSAT-3DR and GNSS retrievals matchup criteria

The assessment of accuracy of INSAT-3DR satellite retrieved IPWV with 19 GNSS stations in different geographical locations which are located in coastal, inland and desert regions over the Indian subcontinent and are shown in Table 2. The GNSS IPWV data sampled every 15 minute and to maintain consistency with INSAT-3DR retrievals that are available every one hour interval of time over the Indian region for the period 1st January 2017 to 30th June 2018 have been utilized. Matchup data sets for were prepared for INSAT-3DR and GNSS IPWV as per the following criteria

(1) To reduce the local horizontal gradient arising in IPWV, The absolute distance between the position of the GNSS stations locations are set within the 0.25° latitude and longitude of the INSAT-3DR retrievals in the region surrounding the stations.

(2) The temporal resolution selected of INSAT-3DR and 19 GNSS observations is within 30 min time interval depending on retrievals and the location of the GNSS stations.

(3) The INSAT-3DR IPWV retrievals are interpolated to different geographical locations of 19 GNSS observations.

Table 3. Statistical analysis of IPWV retrievals from INSAT-3DR & GNSS data (January-2017 & June-2018).

S. No	Station	N	MB (mm)	RMSE (mm)	R
1	ARGD	2318	-0.99	4.83	0.85
2	BHPL	791	3.48	5.88	0.93
3	DBGH	688	-3.02	12.38	0.72
4	DELH	1880	-1.58	4.53	0.89
5	NGPR	2032	-0.10	4.32	0.89
6	JBPR	952	1.96	4.39	0.93
7	JIPR	1576	0.46	4.26	0.88
8	JPGI	1551	2.25	8.10	0.75
9	PUNE	567	0.69	6.18	0.83
10	RIPR	1849	0.71	4.01	0.84
11	BWNR	1443	1.51	5.61	0.88
12	DWRK	2628	2.93	7.10	0.85
13	GOPR	1850	0.76	7.59	0.82
14	KRKL	1128	0.52	6.59	0.88
15	KYKM	1574	1.91	7.21	0.80
16	MPTM	1747	3.12	7.29	0.81
17	TRVM	905	0.01	7.56	0.76
18	PNJM	1396	-2.93	9.28	0.67
19	SGGN	1040	-1.41	4.42	0.88

Table 4. Statistical seasonal analysis of retrievals of IPWV from INSAT-3DR and GNSS data

Station	Season	N	MB (mm)	RMSE (mm)	R
ARGD	Pre Monsoon (MAM)	1129	-2.10	4.14	0.86
	Monsoon (JJA)	73	-0.53	5.50	0.49
	Post Monsoon (SON)	271	3.02	6.23	0.90
	Winter (DJF)	845	-0.84	5.10	0.67
BHPL	Pre Monsoon (MAM)	69	-0.49	3.81	0.77

	Monsoon (JJA)	78	2.10	7.73	0.64
	Post Monsoon (SON)	339	5.23	6.96	0.93
	Winter (DJF)	305	2.78	4.16	0.95
DBGH	Pre Monsoon (MAM)	214	-1.96	6.69	0.72
	Monsoon (JJA)	83	-12.39	14.71	0.64
	Post Monsoon (SON)	79	-22.52	27.74	-0.28
	Winter (DJF)	312	3.68	7.39	0.48
DELH	Pre Monsoon (MAM)	793	-1.44	3.98	0.85
	Monsoon (JJA)	84	-5.79	7.90	0.92
	Post Monsoon (SON)	230	-0.76	5.13	0.92
	Winter (DJF)	773	-1.51	4.36	0.79
NGPR	Pre Monsoon (MAM)	772	-1.42	4.06	0.85
	Monsoon (JJA)	25	0.39	5.41	0.57
	Post Monsoon (SON)	254	1.08	5.86	0.90
	Winter (DJF)	981	0.61	4.00	0.83
JBPR	Pre Monsoon (MAM)	438	1.51	4.79	0.84
	Monsoon (JJA)	11	-4.05	4.43	0.92
	Post Monsoon (SON)	50	1.89	3.94	0.98
	Winter (DJF)	453	2.54	4.02	0.94
JIPR	Pre Monsoon (MAM)	505	-0.44	3.86	0.83
	Monsoon (JJA)	70	-3.84	5.89	0.92
	Post Monsoon (SON)	383	1.34	4.48	0.89
	Winter (DJF)	618	1.13	4.21	0.71
JPGI	Pre Monsoon (MAM)	527	-1.59	6.88	0.79
	Monsoon (JJA)	67	-6.69	9.25	0.75
	Post Monsoon (SON)	161	9.43	10.91	0.65
	Winter (DJF)	796	4.09	8.07	0.50
PUNE	Pre Monsoon (MAM)	333	0.03	6.65	0.72
	Monsoon (JJA)	63	-3.10	5.09	0.67
	Post Monsoon (SON)	170	3.35	5.54	0.79
	Winter (DJF)	1	5.90	5.90	NaN
RIPR	Pre Monsoon (MAM)	864	-0.39	3.94	0.84
	Monsoon (JJA)	0	NaN	NaN	NaN
	Post Monsoon (SON)	68	4.83	6.09	0.75
	Winter (DJF)	917	1.45	3.88	0.77
KRKL	Pre Monsoon (MAM)	739	0.03	5.29	0.89
	Monsoon (JJA)	105	-0.58	8.54	0.15
	Post Monsoon (SON)	31	-1.88	8.54	0.59
	Winter (DJF)	253	2.68	8.53	0.63
KYKM	Pre Monsoon (MAM)	686	0.31	5.84	0.79

	Monsoon (JJA)	110	-1.73	9.53	0.31
	Post Monsoon (SON)	155	0.88	11.21	0.50
	Winter (DJF)	623	4.56	6.83	0.88
MPTM	Pre Monsoon (MAM)	767	2.17	5.54	0.81
	Monsoon (JJA)	40	2.47	5.22	0.77
	Post Monsoon (SON)	172	-0.43	13.49	0.48
	Winter (DJF)	768	4.89	6.94	0.73
GOPR	Pre Monsoon (MAM)	837	-1.22	7.11	0.70
	Monsoon (JJA)	29	-2.25	4.23	0.88
	Post Monsoon (SON)	253	1.55	11.41	0.69
	Winter (DJF)	731	2.87	6.48	0.72
DWRK	Pre Monsoon (MAM)	1119	1.42	7.12	0.62
	Monsoon (JJA)	377	-0.93	5.47	0.78
	Post Monsoon (SON)	362	6.09	8.37	0.87
	Winter (DJF)	770	5.54	7.12	0.82
PNJM	Pre Monsoon (MAM)	878	-4.75	10.27	0.60
	Monsoon (JJA)	46	-0.39	5.76	0.60
	Post Monsoon (SON)	39	-6.10	18.73	0.20
	Winter (DJF)	433	0.79	5.35	0.64
TRVM	Pre Monsoon (MAM)	360	-1.85	6.98	0.75
	Monsoon (JJA)	53	-7.05	11.36	0.10
	Post Monsoon (SON)	113	-0.32	10.56	0.42
	Winter (DJF)	379	2.87	6.25	0.82
BWNR	Pre Monsoon (MAM)	441	0.39	5.71	0.80
	Monsoon (JJA)	12	-5.22	7.37	0.89
	Post Monsoon (SON)	92	3.56	8.36	0.79
	Winter (DJF)	898	1.94	5.16	0.82
SGGN	Pre Monsoon (MAM)	179	-1.23	3.81	0.79
	Monsoon (JJA)	33	-3.96	5.49	0.91
	Post Monsoon (SON)	432	-3.24	5.52	0.87
	Winter (DJF)	396	0.72	2.99	0.91

Table 5. Statistical analysis of IPWV retrievals from CAMS & GNSS data (January to December 2018)

S.No.	Station	N	MB (mm)	RMSE (mm)	R
1	ARGD	1624	-2.72	3.69	0.97
2	BHPL	0	NaN	NaN	NaN
3	DBGH	1002	2.91	6.7	0.95
4	DELH	2345	-1.27	3.09	0.99

5	NGPR	1325	1.99	9.17	0.88
6	RIPR	1727	-1.94	3.48	0.98
7	JBPR	1483	-1.11	3.25	0.99
8	PUNE	1165	-6.69	7.62	0.96
9	JIPR	1483	0.75	7.19	0.92
10	JPGI	2168	-0.68	3.83	0.98
11	BWNR	1240	7.5	13.59	0.48
12	KRKL	1949	-0.9	3.74	0.96
13	KYKM	2145	0.47	3.33	0.96
14	MPTM	1929	-1.3	3.69	0.97
15	PNJM	750	2.27	7.25	0.78
16	GOPR	1625	-0.41	3.76	0.98
17	DWRK	2094	-0.87	3.12	0.98
18	TRVM	2073	-1.91	4.33	0.93
19	SGGN	2274	-1.74	3.37	0.98

Table 6.Statistical seasonal analysis of retrievals of IPWV from CAMS and GNSS data

Station	Season	N	MB (mm)	RMSE(mm)	R
ARGD	Pre Monsoon (MAM)	673	-2.09	3.25	0.93
	Monsoon (JJA)	97	-3.02	5.32	0.75
	Post Monsoon (SON)	248	-3.42	4.24	0.97
	Winter Winter (DJF)	606	-3.09	3.6	0.96
BHPL	Pre Monsoon (MAM)	0	NaN	NaN	NaN
	Monsoon (JJA)	0	NaN	NaN	NaN
	Post Monsoon (SON)	0	NaN	NaN	NaN
	Winter (DJF)	0	NaN	NaN	NaN
DBGH	Pre Monsoon (MAM)	261	5.98	7.48	0.92
	Monsoon (JJA)	169	6.6	7.43	0.84
	Post Monsoon (SON)	396	1.39	6.37	0.95
	Winter (DJF)	176	-1.76	5.31	0.49
DELH	Pre Monsoon (MAM)	719	-0.86	2.83	0.95
	Monsoon (JJA)	223	0.2	4.9	0.92
	Post Monsoon (SON)	721	-2.22	3.57	0.99
	Winter (DJF)	682	-1.19	1.74	0.97
NGPR	Pre Monsoon (MAM)	192	-0.53	2.27	0.94
	Monsoon (JJA)	211	1.57	3.53	0.89
	Post Monsoon (SON)	410	7.23	16.06	0.5

	Winter (DJF)	512	-1.09	2	0.97
JBPR	Pre Monsoon (MAM)	276	1.49	3.48	0.86
	Monsoon (JJA)	160	0.97	2.8	0.9
	Post Monsoon (SON)	507	-2.52	3.89	0.98
	Winter (DJF)	540	-1.72	2.5	0.96
JIPR	Pre Monsoon (MAM)	276	3.67	8.28	0.16
	Monsoon (JJA)	160	2.28	7.53	0.73
	Post Monsoon (SON)	507	-0.47	8.05	0.88
	Winter (DJF)	540	-0.05	5.4	0.58
JPGI	Pre Monsoon (MAM)	662	0.69	4.15	0.93
	Monsoon (JJA)	188	-2.79	4.41	0.8
	Post Monsoon (SON)	644	-1.58	4.32	0.97
	Winter (DJF)	674	-0.57	2.63	0.87
PUNE	Pre Monsoon (MAM)	456	-7.28	8.21	0.92
	Monsoon (JJA)	212	-7.06	8.02	0.81
	Post Monsoon (SON)	424	-6.32	7.14	0.94
	Winter (DJF)	73	-4.1	4.65	0.94
RIPR	Pre Monsoon (MAM)	573	-0.98	3.59	0.94
	Monsoon (JJA)	135	-1.94	3.53	0.74
	Post Monsoon (SON)	488	-2.79	3.96	0.98
	Winter (DJF)	531	-2.21	2.81	0.97
KRKL	Pre Monsoon (MAM)	711	-1.28	3.37	0.97
	Monsoon (JJA)	225	0.52	2.94	0.8
	Post Monsoon (SON)	690	-0.8	4.37	0.89
	Winter (DJF)	323	-1.26	3.58	0.95
KYKM	Pre Monsoon (MAM)	647	0.61	3.44	0.94
	Monsoon (JJA)	212	0.03	3.01	0.87
	Post Monsoon (SON)	589	1.07	3.57	0.92
	Winter (DJF)	697	-0.03	3.11	0.95
MPTM	Pre Monsoon (MAM)	632	-0.28	3.26	0.94
	Monsoon (JJA)	223	0.96	3.31	0.8
	Post Monsoon (SON)	655	-2.26	4.27	0.96
	Winter (DJF)	419	-2.55	3.52	0.96
DWRK	Pre Monsoon (MAM)	597	-1.02	2.53	0.91
	Monsoon (JJA)	218	1.42	3.4	0.96
	Post Monsoon (SON)	614	-0.92	3.8	0.95
	Winter (DJF)	665	-1.43	2.77	0.91
GOPR	Pre Monsoon (MAM)	656	-1.4	4.46	0.89
	Monsoon (JJA)	231	2.1	3.65	0.8
	Post Monsoon (SON)	318	1.42	3.35	0.96
	Winter (DJF)	420	-1.64	2.78	0.92

PNJM	Pre Monsoon (MAM)	398	3.6	7.88	0.74
	Monsoon (JJA)	75	3.57	11.41	0.38
	Post Monsoon (SON)	277	0.01	4.23	0.86
	Winter (DJF)	0	NaN	NaN	NaN
TRVM	Pre Monsoon (MAM)	631	-2.26	4.7	0.9
	Monsoon (JJA)	199	-0.51	2.3	0.92
	Post Monsoon (SON)	617	-1.17	3.85	0.89
	Winter (DJF)	626	-2.74	4.84	0.89
BWNR	Pre Monsoon (MAM)	644	13.88	16.5	0.29
	Monsoon (JJA)	0	NaN	NaN	NaN
	Post Monsoon (SON)	0	NaN	NaN	NaN
	Winter (DJF)	596	0.6	9.48	0.16
SGGN	Pre Monsoon (MAM)	680	-0.85	2.76	0.93
	Monsoon (JJA)	192	-0.84	4.57	0.94
	Post Monsoon (SON)	712	-2.51	4.04	0.97
	Winter (DJF)	690	-2.05	2.67	0.95

3. Results and discussion

3.1 Inter-comparison of INSAT-3DR and Indian GNSS IPWV

From Figure 3, The Taylor diagram to evaluate the skill characteristics of the annual distribution of IPWV retrieved from INSAT-3DR satellite with 19 GNSS IPWV at different geographical locations (Figure 2) over Indian subcontinent during the period of 1 January 2017 to 30 June 2018. Further tailor diagram displaying three statically skill metrics: distribution of the correlation coefficient, root mean square error (RMSE) and standard deviation. If an IPWV performs nearly perfectly, its position in the diagram is expected to be very close to the observed point (Figure 3). An attempt have been made to evaluate the IPWV retrieved from INSAT-3DR satellite with GNSS observations show the root mean square error (RMSE) of 8 inland stations out of 10 stations lies between 4 to 6 mm except 8 mm and 12 mm for Jalpaiguri (JPGI) and Dibrugarh (DBGH) stations respectively. The observation points in case of Dibrugarh (DBGH) are more symmetrical (or association) than Jalpaiguri (JPGI) even RMSE values are higher (Figure 4).The value of Correlation Coefficient (CC) and bias for inland stations lie in the range (0.72 to 0.93) & (-3.0 mm to +3.0 mm) respectively. Similarly, for all the coastal stations the value of CC and bias lie in the range (0.67 to 0.88) & (-3.0 mm to +3.0 mm) respectively. RMSE for 7 coastal stations out of 8 stations lie between 5 mm to 7 mm except 9 mm of Panjim. The value of CC and bias and RMSE for desert station (SGGN) 0.88, -1.4 mm and 4.42 mm respectively (Table 3).

The correlation coefficient of IPWV varies from 0.60 to 0.89 of all the stations for the pre monsoon season. IPWV retrieved from INSAT-3DR satellite with respect to GNSS IPWV are having the negative biases ranges (-6.7 mm to -0.39 mm) which are indicating underestimation of IPWV at the stations of ARGD, DBGH, DELH, NGPR, JIPR, JPGI, RIPR, GOPR, PNJM, TRVM &

SGGN. The stations JBPR, PUNE, KRKL, KYKM, MPTM, DWRK, and BWNR are having the positive biases ranges (0.03 to 2.54 mm) which are indicating overestimation of IPWV by INSAT-3DR during pre-monsoon season. RMSE ranges between 3.5 mm to 10 mm (Table 4).

The correlation coefficient of IPWV varies from 0.60 to 0.90 of all the stations during monsoon season except TRVM (0.1), KYKM (0.31) and KRKL (0.15) respectively. The stations ARGD, DBGH, DELH, JBPR, JIPR, JPGI, PUNE, KRKL, KYKM, GOPR, BWNR, PNJM, TRVM and SGGN are having the negative biases ranges (-0.39 mm to -12.39 mm) which are indicating the underestimation of IPWV by INSAT-3DR as compared to MPTM, NGPR & BHPL are having the positive biases ranges of (0.39 mm to 2.47 mm) during monsoon season. RMSE ranges of 4.23 mm to 14.71 mm (Table 4).

The correlation coefficient of IPWV varies from 0.60 to 0.98 of all the stations during post monsoon season except TRVM (0.42), PNJM (0.2), MPTM (0.48), KYKM (0.50) and DBGH (-0.28) respectively. The stations DBGH, DELH, KRKL, MPTM, PNJM, TRVM and SGGN are having the negative biases ranges (-0.32 mm to -6.10 mm) except DBGH (-22.52 mm) which are indicating the underestimation of IPWV by INSAT-3DR as compared to ARGD, BHPL, NGPR, JBPR, JIPR, JPGI, PUNE, RIPR, KYKM, GOPR, DWRK, BWNR are having the positive biases ranges of (0.88 mm to 9.43 mm) during post-monsoon season. RMSE ranges from 3.94 mm to 13.49 mm except PNJM (18.73 mm) & DBGH (27.74 mm) respectively (Table 4).

The correlation coefficient of IPWV varies from 0.64 to 0.95 of all the stations during winter season except DBGH (0.48), JPGI (0.50) respectively. The stations BHPL, DBGH NGPR, JBPR, JIPR, JPGI, PUNE, RIPR, KRKL, KYKM, MPTM, GOPR, DWRK, PNJM, TRVM, BWNR & SGGN are having the positive biases ranges (0.61mm to 5.90) which are indicating the overestimation of IPWV by INSAT-3DR as compared to ARGD (-0.84 mm) & DELH (-1.51mm) during winter season. RMSE ranges of 2.99 mm to 8.53mm (Table 4).

Scatter plot of hourly INSAT-3DR IPWV and GNSS IPWV plotted in Figure 4 using hexagonal binning. The number of occurrences in each bin is colour-coded (not on a linear scale). It is now possible to see where most of the data lie and a better indication of the relationship between GNSS IPWV and INSAT-3DR IPWV are revealed.

Stations TRVM, KYKM, KRKL, PNJM, MPTM, JPGI and DBGH are poorly correlated (INSAT-3DR vs. GNSS) averaging of INSAT-3DR pixels in gridded data contains both sea and mountainous land together along with topographically diverse terrains around these stations. Similar behavior is also seen in annual analysis of IPWV in coastal stations with the above said reasons.

It is seen that discrepancies arise because the wet mapping functions that used to map the wet delay at any angle to the zenith do not represent the localized atmospheric condition particularly for Narrow towering thunder clouds and non-availability of GPS satellites in the zenith direction (Puviarasan et al., 2020).

Large or small bias between IPWV retrieved from INSAT-3DR and GNSS exists due to limitations of the INSAT-3DR retrievals and calibration uncertainties in the radiance measured by INSAT-3DR. Another possibility of operation differences in IPWV measurements adopted in GNSS /INSAT-3DR in respect to mapping functions /weighting functions.

The results indicate that the RMSE values increases significantly under the wet conditions (Pre Monsoon & Monsoon season) than under dry conditions (Post Monsoon & winter season) (Table 4).The study showed differences in the magnitude and sign of bias of INSAT-3DR with respect to GNSS IPWV from station to station and season to season. The data quality of INSAT-3DR IPWV may be improved due to proper bias correction coefficient applied before physical retrievals of IPWV during clear sky pixels.

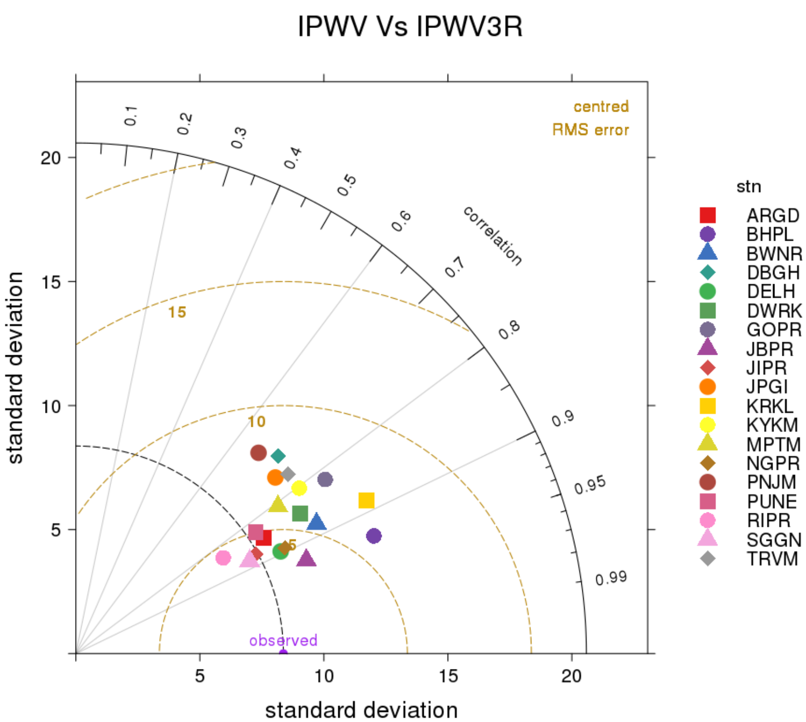

Figure 3. Taylor diagram of INSAT-3DR vs. Indian GNSS retrievals.

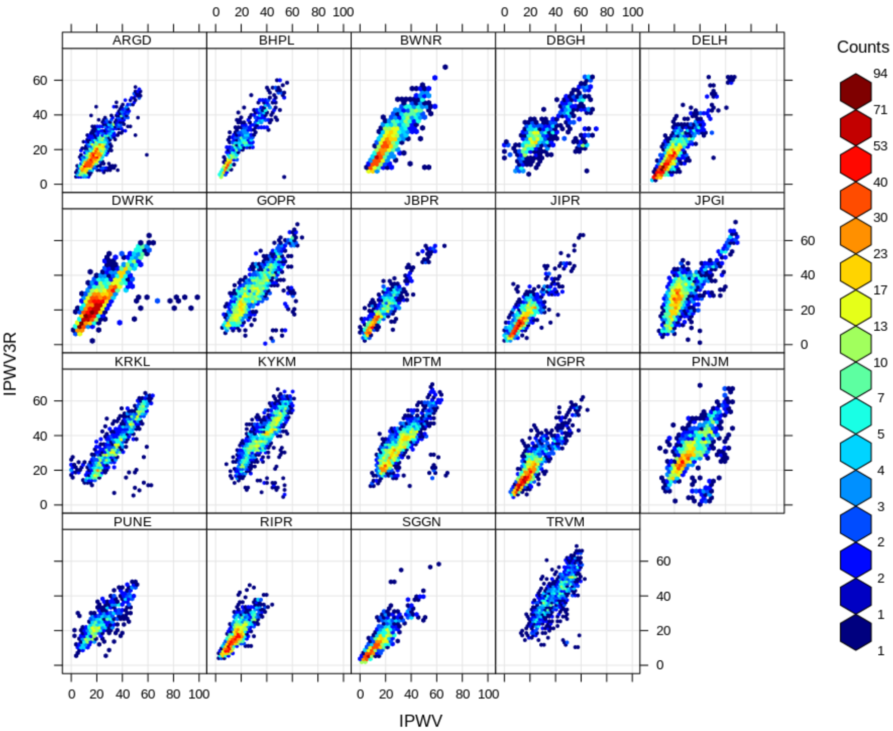

Figure 4. Scatter plot of hourly INSAT-3DR IPWV vs. GNSS IPWV using hexagonal binning.

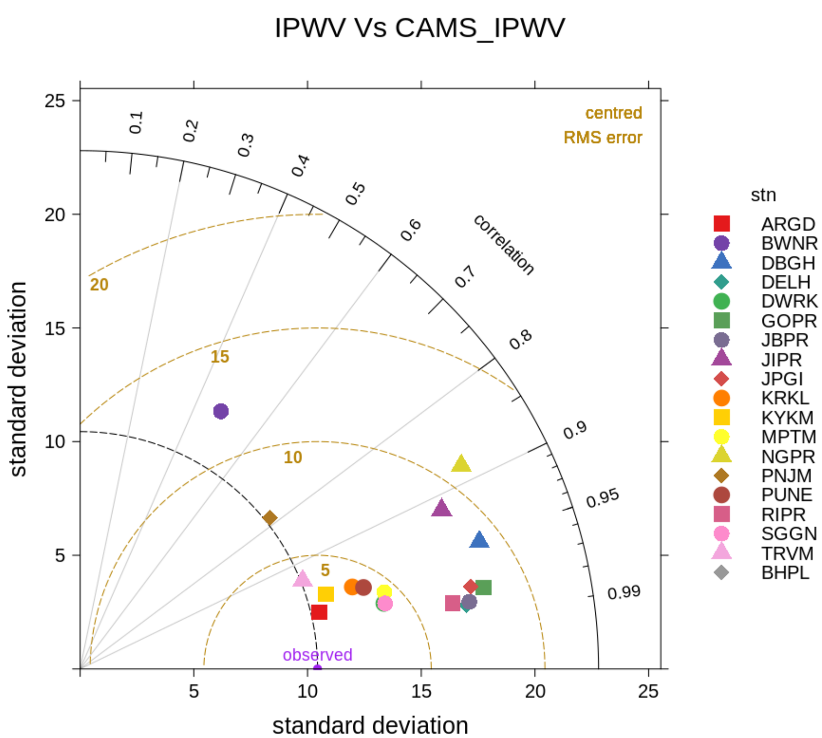

Figure 5.Taylor diagram of CAMS vs. Indian GNSS retrievals.

3.2 Inter-comparison of CAMS reanalysis and Indian GNSS IPWV

From the Figure 5, the Taylor diagram evaluates the skill characteristics in terms of RMSE, Correlation Coefficient and Standard Deviation of the annual distribution of IPWV retrieved from CAMS with 19 GNSS IPWV at different geographical locations (Figure 5) over Indian subcontinent during the period of 1 January 2018 to 31 December 2018. The root mean square error (RMSE) between CAMS reanalysis & GNSS data retrievals of 9 inland stations out of 10 stations lies between 3 to 7 mm except 9 mm for Nagpur (NGPR) station respectively. The value of Correlation Coefficient (CC) and bias for inland stations lie in the range (0.88 to 0.99) & (-3.0 mm to +3.0 mm, except Pune, -6.69 mm) respectively (Table 5).

Root Mean Square Error (RMSE) for 7 coastal stations out of 8 stations lie between 3 to 7 mm except 14.0 mm of Bhubaneswar (BWNR). The value of CC and bias lie in the range (0.78 to 0.98 except 0.48 BWNR) & (-2.0 mm to +2.0 mm except +7.5 mm at BWNR) respectively. The value of CC and bias for desert station (SGGN) 0.88 and -1.4 mm respectively. The desert station RMSE, CC & Bias are 3.37 mm, 0.98 and -1.74 mm respectively (Table 5).

The correlation coefficient of IPWV varies from 0.74 to 0.97 of all the stations except JIPR (0.16) & BWNR (0.29) for the pre monsoon season. IPWV retrieved from CAMS reanalysis with respect to GNSS IPWV are having the negative biases ranges (-7.28 mm to -0.28 mm) which are indicating underestimation of IPWV at the stations of ARGD, DELH, NGPR, PUNE, RIPR, KRKL, MPTM, DWRK, GOPR, TRVM, SGGN. The stations DBGH, JBPR, JIPR, JPGI, KYKM, PNJM and BWNR are having the positive biases ranges (0.61 mm to 13.88 mm) which are indicating overestimation of IPWV by CAMS during pre-monsoon season. RMSE ranges between 2.27 mm to 8.28 mm except BWNR (16.50 mm) (Table 6).

The correlation coefficient of IPWV varies from 0.73 to 0.96 of all the stations during monsoon season except PNJM (0.38) respectively. The stations ARJD, JPGI, PUNE, RIPR, TRVM and SGGN are having the negative biases ranges (-0.51 mm to -7.28 mm) which are indicating the underestimation of IPWV by CAMS reanalysis as compared to DBGH, DELH, NGPR, JBPR, JIPR, KRKL, KYKM, MPTM, DWRK, GOPR & PNJM are having the positive biases ranges of (0.03 mm to 6.60 mm) during monsoon season. RMSE ranges from 2.30 mm to 11.41 mm. Data is not available at the stations of BHPL & BWNR (Table 6).

The correlation coefficient of IPWV varies from 0.86 to 0.99 of all the stations during post monsoon season except NGPR (0.50) respectively. The stations ARJD, DELH, JBPR, JIPR, JPGI, PUNE, RIPR, KRKL, MPTM, DWRK, TRVM, SGGN are having the negative biases ranges (-0.47 mm to -6.32 mm) which are indicating the underestimation of IPWV by CAMS reanalysis as compared to DBGH, NGPR, KYKM, GOPR, PNJM are having the positive biases ranges of (0.01 mm to 7.23 mm) during post-monsoon season. RMSE ranges from 3.35 mm to 8.05 mm except NGPR (16.06 mm) respectively (Table 6). During this transition time most parts of the Indian region remain gradually dry and decrease in water content as compared to the North East and

Southern parts of India. It has been observed in this analysis during post-monsoon season, stations located in dry/wet regions of India CAMS data under/over estimates with respect to GNSS.

The correlation coefficient of IPWV varies from 0.87 to 0.97 of all the stations during winter season except DBGH (0.49) JIPR (0.58) & BWNR (0.16) respectively. The stations ARJD, DBGH, DELH, NGPR, JBPR, JIPR, JPGI, PUNE, RIPR, KRKL, KYKM, MPTM, DWRK, GOPR, TRVM, SGGN are having the negative biases ranges (-0.03 mm to -4.10 mm) which are indicating the underestimation of IPWV by CAMS reanalysis as compared to BWNR are having the positive biases of (0.60 mm) during winter season. RMSE ranges of 1.74 mm to 9.48 mm respectively (Table 6).

During winter season over Indian region, local effects which play an important role moisture development are suppressed from their importance due to sparse observation network data and optimization of random and systematic errors which is further utilized for effective improvement in model predictions (Inness et al., 2019).

CAMS data used in this study have consistency and homogeneous spatial with reduced bias and better performance of model physics and dynamics due to assimilation of new data sets (Inness et al., 2019). But over Indian domains during pre-monsoon season land stations are mainly affected by local convective developments of shorter time scale of a few hours which is not captured by the CAMS data and a dry bias prevails in most of the stations mentioned above.

Few GNSS data is assimilated for Indian region in the latest CAMS Data sets. During monsoon season 6 stations mentioned above are underestimating IPWV with CAMS data due to complex and rugged topographic terrains which are not well captured in CAMS data due to very few observations are available in these locations. In almost all other stations IPWV values are overestimated as the global features of monsoon flow are well captured by the CAMS data. The similar findings (overestimate or underestimate) are also observed with GNSS data for above mentioned stations except PNJM and BWNR where the meteorological sensor gets replaced 2 to 3 times during the year of 2018. Standard deviation (SD) between CAMS reanalysis and Indian GNSS retrievals is more dispersed from their mean values (Figure 5).

3.3 Inter-comparison of CAMS reanalysis and INSAT-3DR IPWV

The correlation coefficient (CC) computed between INSAT-3DR and CAMS reanalysis, IPWV retrievals are negatively correlated in almost entire the land area, except pockets of Indo Gangetic Plain (IGP) of Indian region for winter months. The computed value of CC lies within the range 0.2 to -0.5 in the land area. Over Ocean retrievals the values of CC are slightly positive side (0.0 to 0.5) in the entire area of Bay of Bengal and Arabian Sea except off shore area on both east and west side in winter months (Figure 6). This poor resemblance between the results (INSAT-3DR and CAMS) may be due to the interpolated values of coarser resolution CAMS data.INSAT-3DR satellite based data have diverse, covariant information content, different temporal coverage and have smaller ability with respect to representative observations in CAMS.

In pre-monsoon season the value of CC between INSAT-3DR and CAMS reanalysis retrievals is positive (0.0 to 0.6) over Oceanic entire areas of Bay of Bengal and Arabian Sea except few patches in Arabian Sea. Over land the values are slightly positive (0.0 to 0.2) in many areas and slightly negative (0.0 to -0.3) for pockets of the North West and Central India region (Figure 6).

During monsoon month the value of CC over land area are mostly positively correlated (0.0 to 0.7) except the belt of monsoon trough and south India which have shown appreciably low value of CC (-0.3 to -0.5). This might be due to the presence of clouds on both sides of monsoon trough and southern belt of India during monsoon season. (Figure 6).

In post monsoon season months the value of CC between INSAT-3DR and CAMS reanalysis retrievals are positive (0.0 to 0.7) for both land and oceanic areas almost entirely except some areas of North of Bay and Bengal and South East Arabian Sea (Figure 6).

The differences in the magnitude and sign of CC of INSAT-3DR with respect to CAMS reanalysis IPWV may be due to lack of assimilation of quality controlled data over Indian domain. This may be due to limitations of the design of the instrument /sensor on board on INSAT-3DR or retrieval algorithm of IPWV. Therefore, it will affect the overall collocations in matchup data sets.

During winter season, positive biases ranges (0.0 to 5.0 mm) observed between CAMS reanalysis and INSAT-3DR IPWV which are indicating overestimation of CAMS IPWV over land and oceanic region except east and west coast of India including Arabian Sea (12º N to 28º N), some pockets of South East Bay of Bengal (BOB) and Himalayan region ranges (-2.5 mm to -5.0 mm) which indicates underestimation of CAMS IPWV respectively (Figure 7).

During pre-monsoon season, positive biases ranges (0.0 to 10.0 mm) observed between CAMS reanalysis and INSAT-3DR IPWV which indicates overestimation of CAMS IPWV over land and oceanic region except some parts of North West of Arabian Sea and Himalayan region ranges (-0.0 mm to -3.0 mm) which indicates underestimation of CAMS IPWV respectively (Figure 7).

During monsoon season, positive biases ranges (2.5 to 10.0 mm) observed between CAMS reanalysis and INSAT-3DR IPWV which indicates overestimation of CAMS IPWV over land and oceanic region except Himalayan region ranges (-2.5 mm to -5.0 mm) which indicates underestimation of CAMS IPWV respectively (Figure 7).

During post monsoon season, positive biases ranges (0.0 to 6.0 mm) observed between CAMS reanalysis and INSAT-3DR IPWV which indicates overestimation of CAMS IPWV over land and oceanic region except Arabian Sea (19^{o} N to 29^{o} N) and Himalayan region ranges (-2.5 mm to -6.0 mm) which indicates underestimation of CAMS IPWV respectively (Figure 7).

The IPWV retrieved from CAMS reanalysis overestimated with respect to INSAT-3DR IPWV over land and oceanic region for all the seasons except Himalayan region and some parts of Arabian Sea and BoB. This occurred because the infrared and microwave radiometer observations of land and oceans had been assimilated into the model, which has the higher systematic humidity when it was compared with Radiosonde data (Andersson et al., 2007). Underestimation of CAMS IPWV compared with INSAT-3DR over Himalayan region may be due to presence of rugged terrain/orographic features in the retrieval of IPWV.

RMSE values during winter season ranges (7.5 mm to 13.0 mm) over land region (20^{o} N to 35^{o} N) and the entire Arabian Sea. Above 35^{o} N latitude including Himalayan region, RMSE values are less than 7.5 mm. RMSE values ranges (13 mm to 20 mm) observed over the Southern peninsula of India and BoB region respectively (Figure 8).

RMSE values during pre-monsoon season ranges (2.5 mm to 13.0 mm) over land region (18^{o} N to 40^{o} N), Arabian Sea and Himalayan region observed. RMSE values ranges (13 mm to 20 mm) are over the Southern peninsula of India, Indo Gangetic Plains (IGP) and BoB region respectively (Figure 8).

RMSE values during monsoon season ranges (14. mm to 20.0 mm) over land region (20^{o} N to 35^{o} N) including North West of Arabian Sea and North East of BoB. Above 35^{o} N latitude, South West & South East of Arabian Sea including South East of BoB and Himalayan region RMSE values are less than 8.0 mm respectively (Figure 8).

RMSE values during post-monsoon season less than 7.5 mm observed over land region including both Arabian Sea as well as BoB region except Indo Gangetic Plains (IGP) and north East of BoB ranges (13 mm to 17 mm) respectively (Figure 8).

Seasonal RMSE between CAMS reanalysis and INSAT-3DR (CAMS-INSAT) retrievals are higher (>15 mm) over Bay of Bengal and pockets of Indo Gangetic Plains (IGP), North East (NE) India, Southern Parts of India, North Indian Ocean and Arabian Sea during pre-monsoon, monsoon, post monsoon season and (< 15 mm) during winter season. Higher values of RMSE prevails over the regions of higher moisture availability or water content in the Atmosphere. (Figure 8).

3.4 Distribution and Variability of IPWV retrieved from INSAT-3DR and CAMS reanalysis

The annual mean value and standard deviation of both the retrievals INSAT -3DR sounder and CAMS reanalysis data sets are presented in Figure 9. The standard deviations of CAMS reanalysis retrieval data set are appreciably high (0.0 to 14 mm) in both land and ocean areas as compared to INSAT-3DR retrievals. This variation of higher spread from mean values may be due to the drier bias present in the CAMS reanalysis data sets (Inness et al, 2019) with coarser resolution as compared to INSAT-3DR retrievals.

The mean IPWV values vary in the range of 0–50 mm depending upon the region and prevailing weather system affected throughout the year. Larger mean IPWVs occur in the coastal regions of Indian Ocean regions compared to inland and desert regions due to warm air conditions as compared to inland and ocean. The south foothill of Himalayas has the largest IPWV variation with a SD ~16 mm (Figure 9). This is attributed to the monsoon season that results in large changes in precipitation at different seasons in these regions. The seasonal distribution of mean IPWV and standard deviation of CAMS and INSAT-3DR for monsoon and post monsoon increased in CAMS data as compared to INSAT -3DR retrievals due to wet bias present in the CAMS data sets (Figure 10).

Over the oceanic region, seasonal mean IPWV of INSAT-3DR and CAMS ranges from 25-40 mm (with standard deviation 6-15 mm) and 20-45 mm (SD 6-16 mm) and less than 25 mm with SD of less than 6 mm for both INSAT-3DR and CAMS IPWV over land region during winter season respectively (Figure 10).

Over the oceanic region, seasonal mean IPWV of INSAT-3DR and CAMS ranges from 30-45 mm (with standard deviation 7-12 mm) and 35-55 mm (SD 10-16 mm). Over land region, seasonal mean IPWV of INSAT-3DR and CAMS data ranges from 15-38 mm with SD of 2-10 and 20-40 mm with SD of 5-12mm during pre-monsoon season respectively (Figure 10).

Seasonal mean IPWV of INSAT-3DR ranges from 30 mm to more than 60 mm with SD of 2-14 mm and from 50 mm to more than 60 mm with SD of 4-16 mm of CAMS IPWV observed for both land and oceans region during monsoon season respectively (Figure 10).

Over the oceanic region, seasonal mean IPWV of INSAT-3DR and CAMS ranges from 35-55 mm (with standard deviation 6-10 mm) and 38-55 mm (SD 6-14 mm) and over land region mean IPWV of INSAT-3DR and CAMS data ranges from 15-35 mm with SD of 5-12 and 20-40 mm with SD of 10-16 mm during post-monsoon season respectively (Figure 10).

The Standard deviations values are higher over ocean as compared to land areas in every season except post monsoon season (Figure 10).

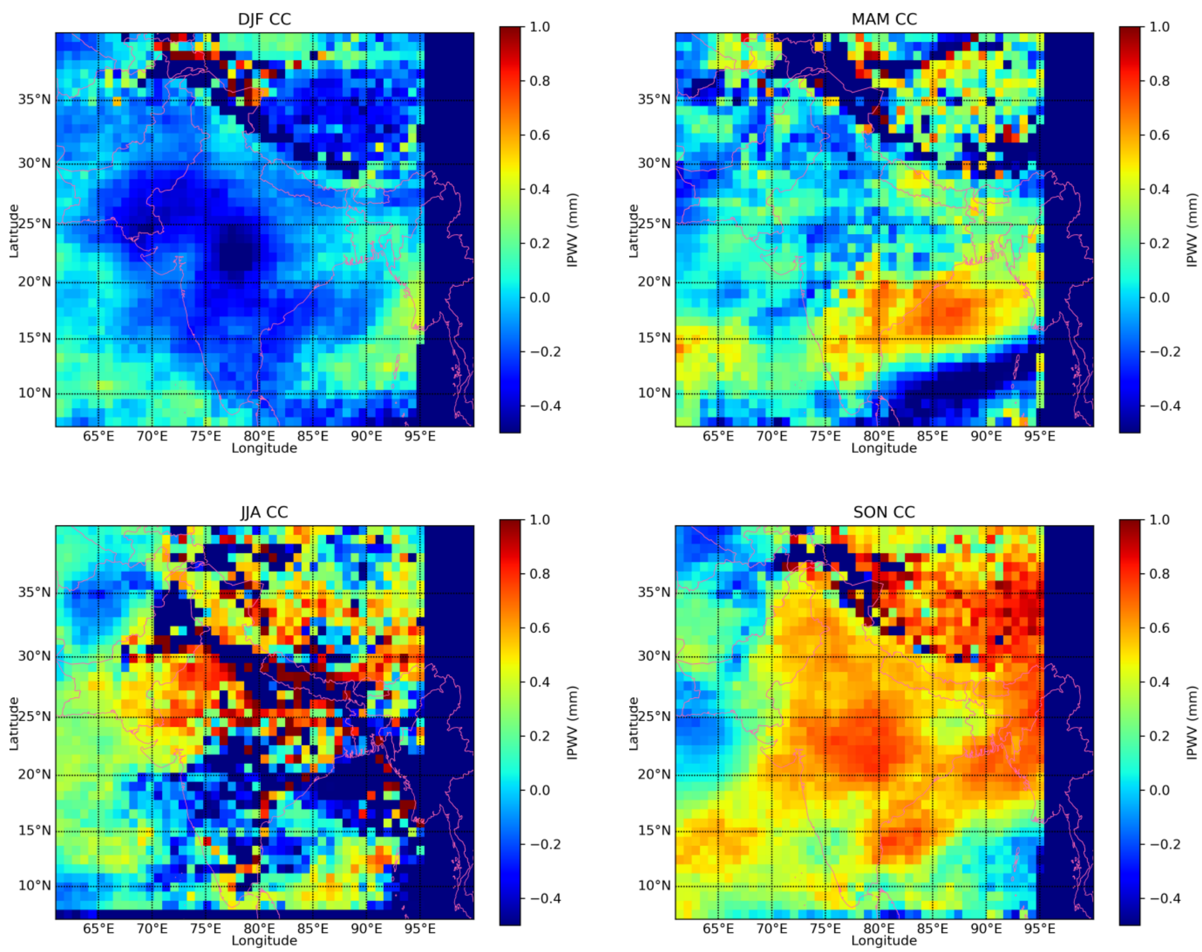

Figure 6. Seasonal Correlation Coefficient of CAMS and INSAT-3DR data

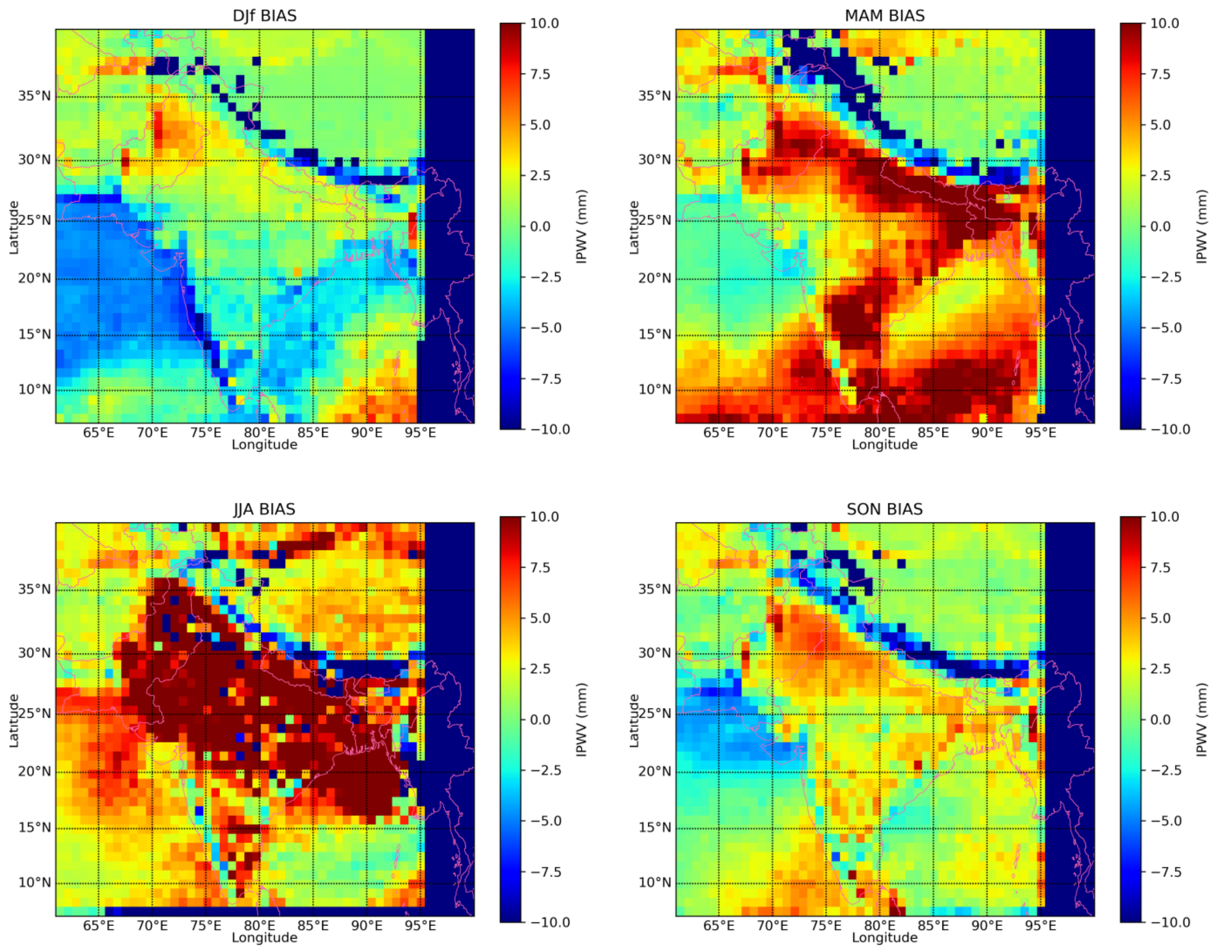

Figure 7. Seasonal bias of IPWV between CAMS and INSAT-3DR

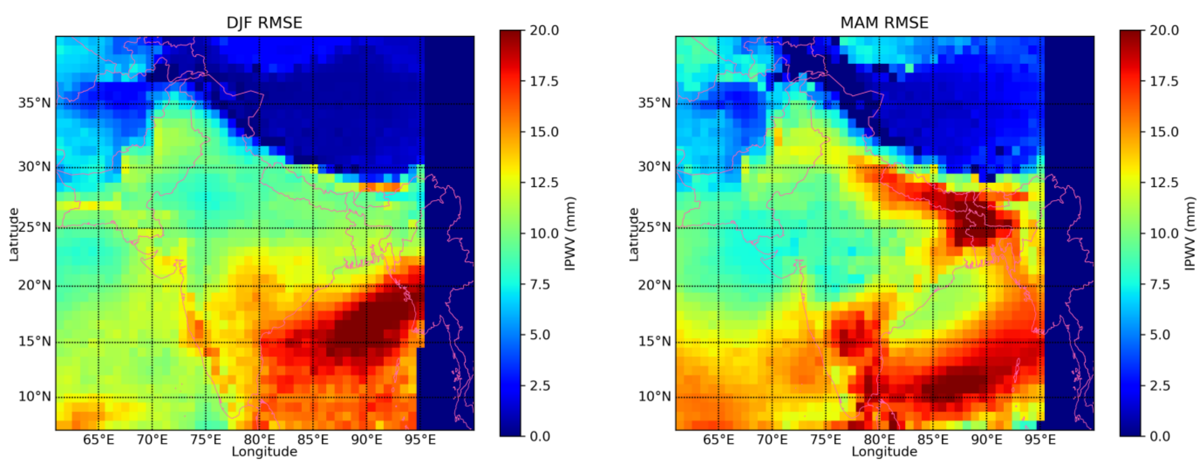

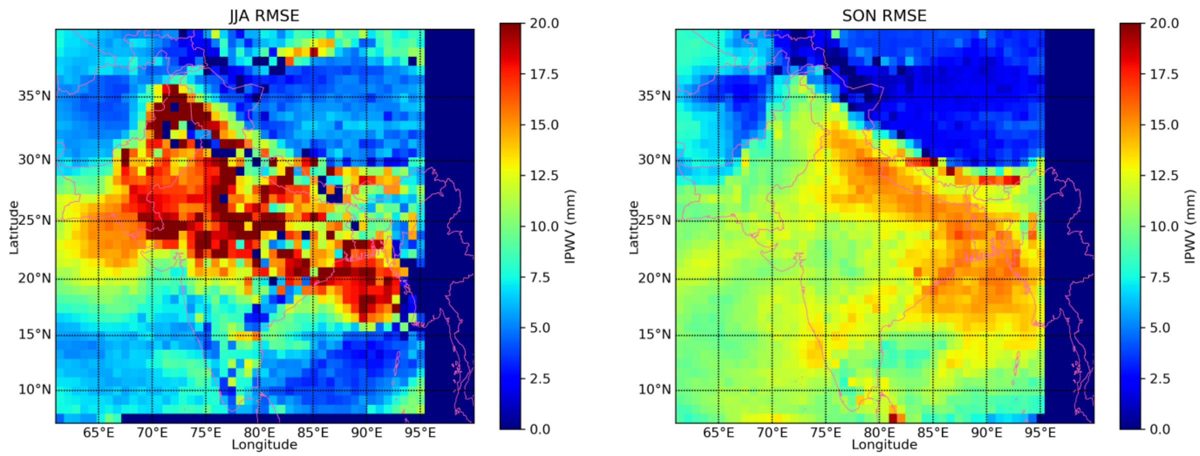

Figure 8. Seasonal RMSE between CAMS and INSAT-3DR

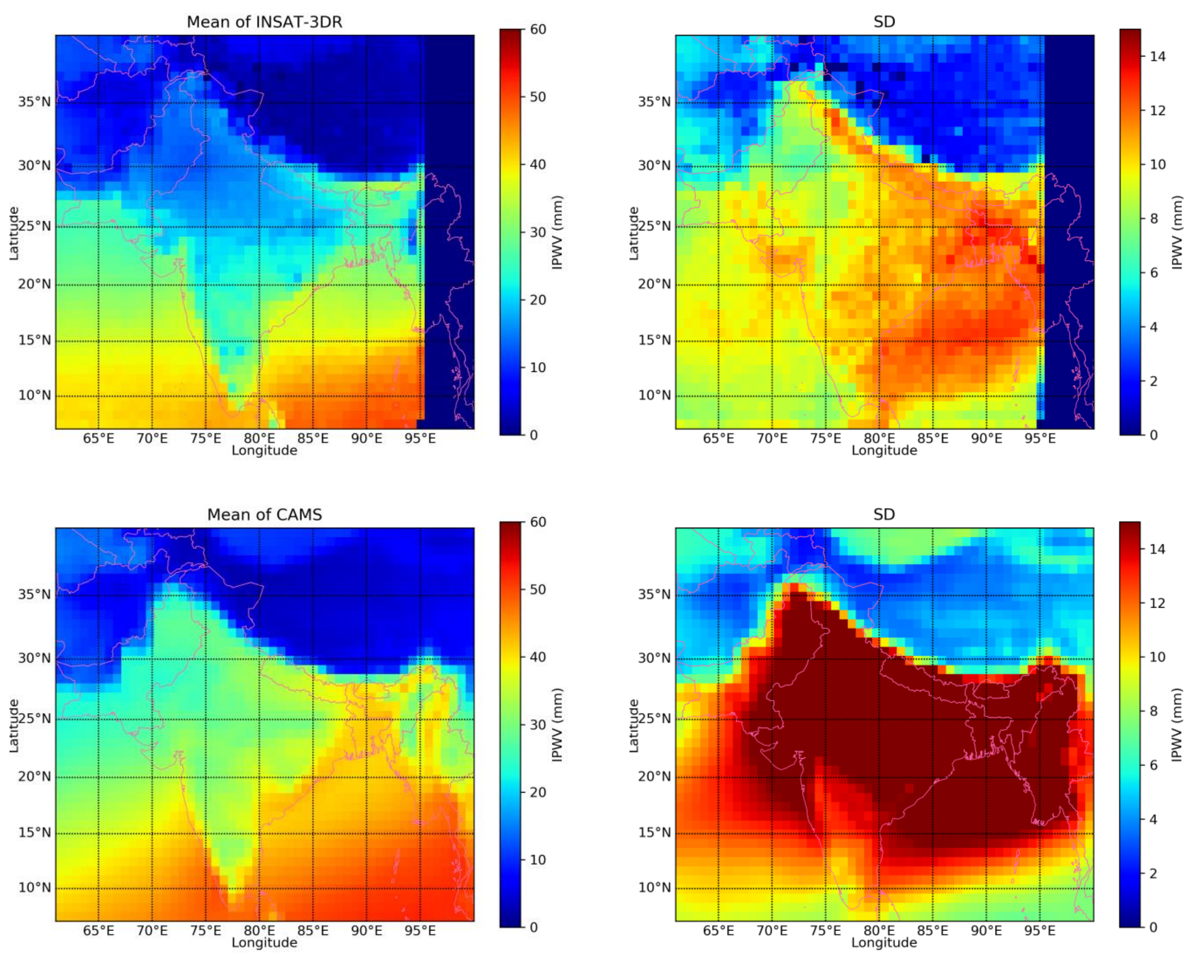

Figure 9. Means and SD of INSAT-3DR and CAMS IPWV for the year 2018

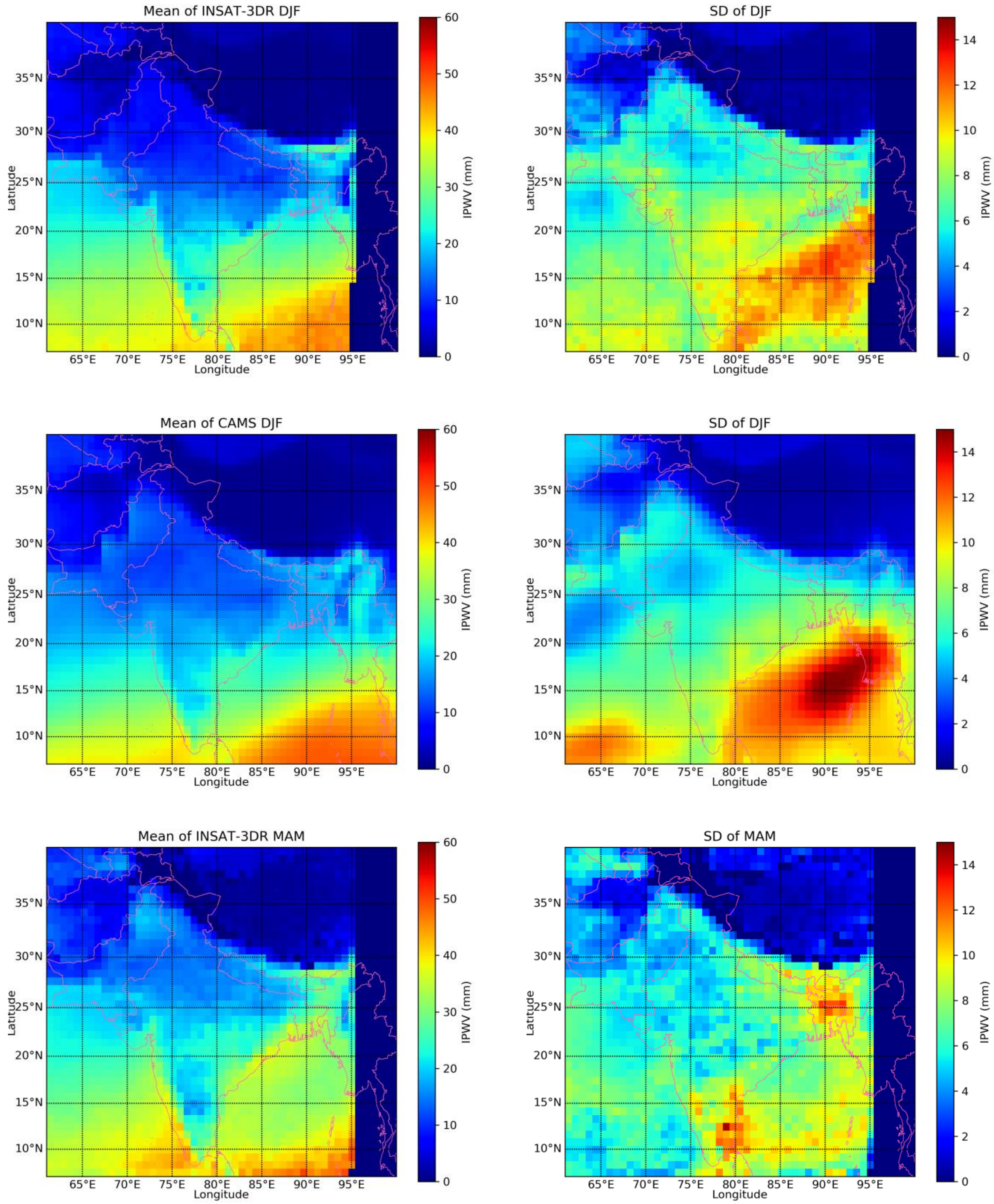
Mean of INSAT-3DR DJF
SD of DJF
Mean of CAMS DJF
SD of DJF
Mean of INSAT-3DR MAM
SD of MAM
Latitude
Longitude
IPWV (mm)
35°N
30°N
25°N
20°N
15°N
10°N
65°E
70°E
75°E
80°E
85°E
90°E
95°E
0
10
20
30
40
50
60
2
4
6
8
10
12
14

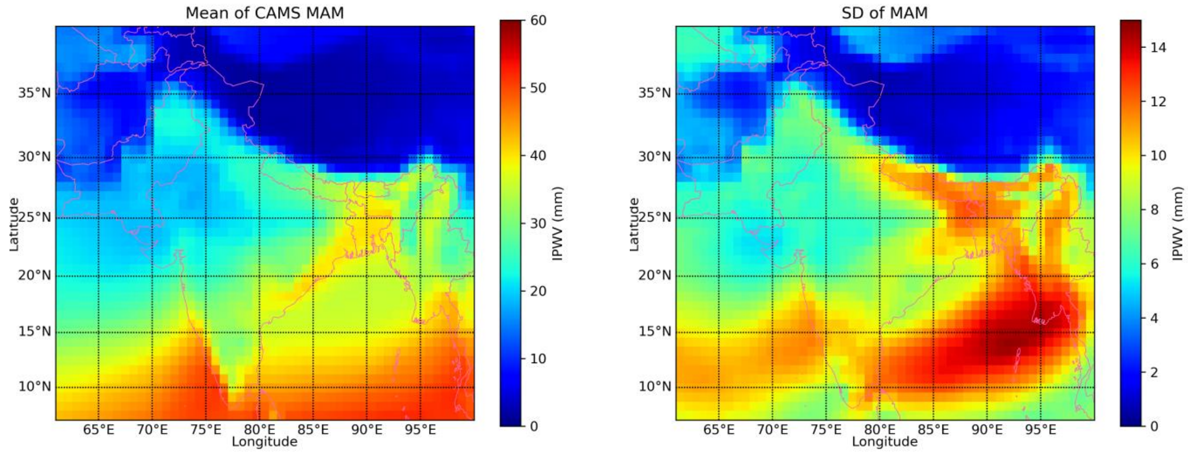
Mean of CAMS MAM
SD of MAM
Latitude
Longitude
IPWV (mm)
35°N
30°N
25°N
20°N
15°N
10°N
65°E
70°E
75°E
80°E
85°E
90°E
95°E

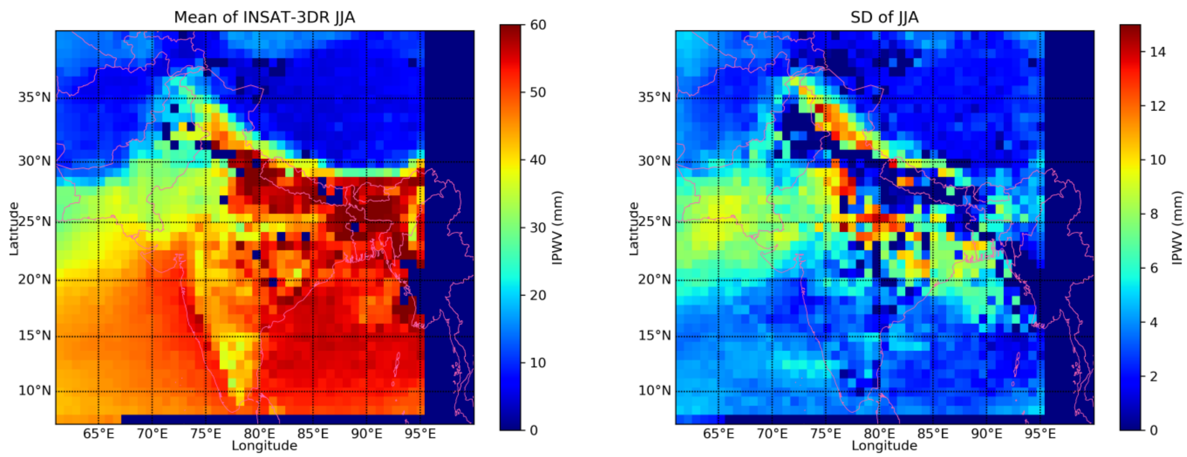
Mean of INSAT-3DR JJA
SD of JJA
Latitude
Longitude
IPWV (mm)
35°N
30°N
25°N
20°N
15°N
10°N
65°E
70°E
75°E
80°E
85°E
90°E
95°E

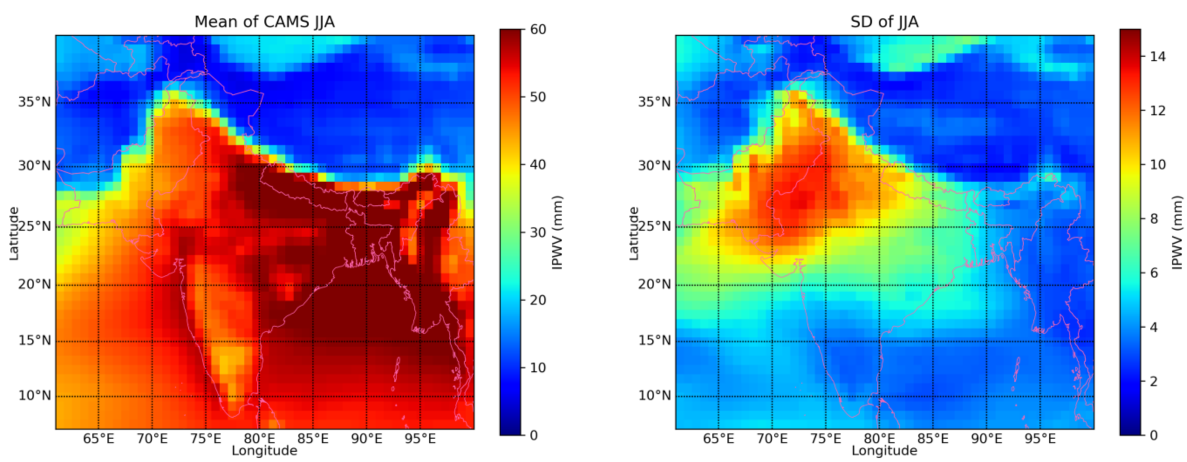
Mean of CAMS JJA
SD of JJA
Latitude
Longitude
IPWV (mm)
35°N
30°N
25°N
20°N
15°N
10°N
65°E
70°E
75°E
80°E
85°E
90°E
95°E

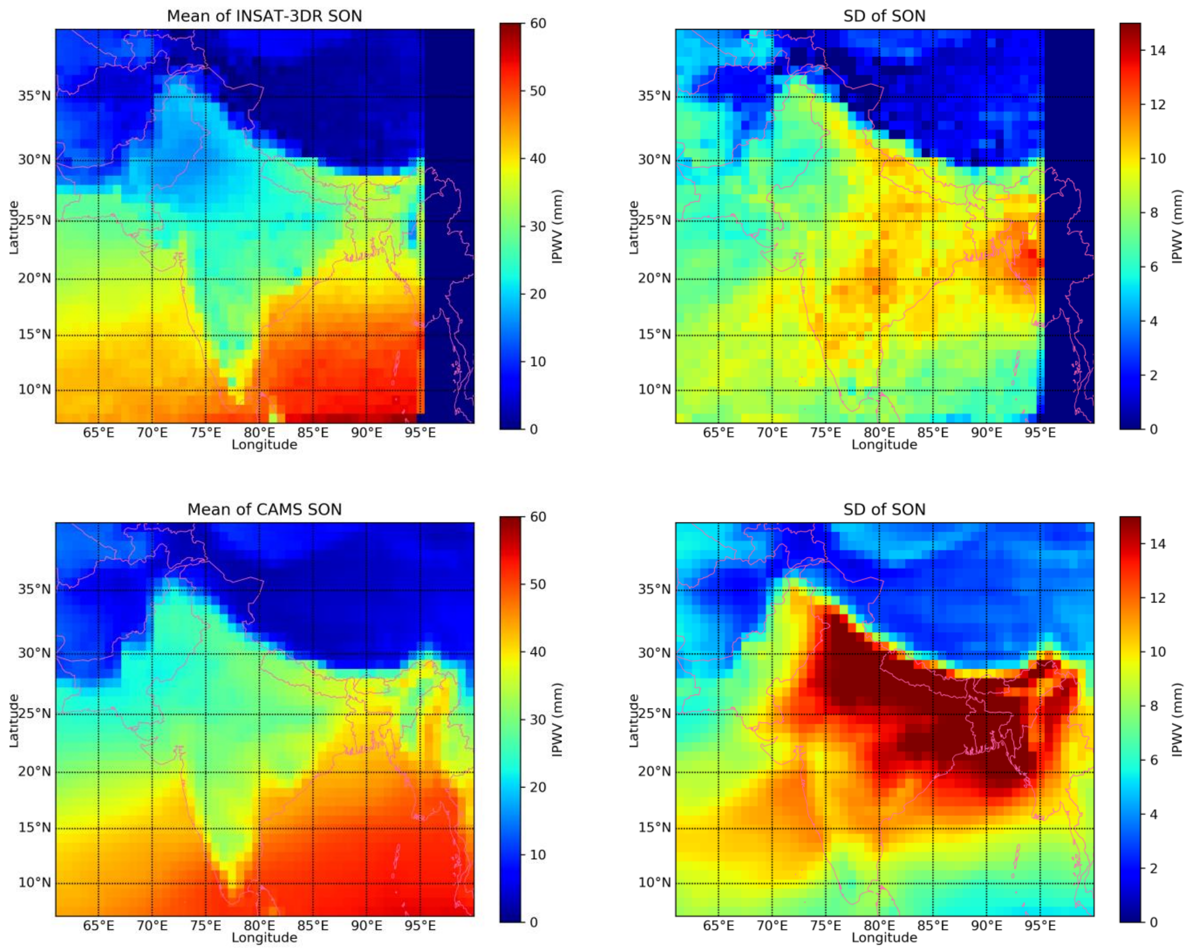

Figure 10. Seasonal Means and SDs of INSAT-3DR and CAMS retrieved IPWV for the year 2018

4. Conclusions

1. It is noticed that seasonal correlation coefficient (CC) values between INSAT-3DR and Indian GNSS data mainly lie within the range of 0.50 to 0.98 for all the selected 19 stations except Thiruvanathpuram (0.1), Kanyakumari (0.31), Karaikal (0.15) during monsoon and Panjim (0.2) during post monsoon season respectively. The seasonal CC values between CAMS and INSAT-3DR IPWV are ranges 0.73 to .99 except Jaipur (0.16) & Bhubneshwar (0.29) during pre-monsoon season, Panjim (0.38) during monsoon, Nagpur (0.50) during post-monsoon and Dibrugarh (0.49) Jaipur (0.58) & Bhubaneswar (0.16) during winter season respectively.
2. The RMSE values increases significantly under the wet conditions (Pre Monsoon & Monsoon season) than under dry conditions (Post Monsoon & winter season) and the differences in magnitude and sign of bias of INSAT-3DR, CAMS with respect to GNSS IPWV from station to station and season to season.

3. Large scale features of moisture flow are generally captured in CAMS reanalysis data except localized features due to sparseness or very few numbers of the quality controlled both ground as well as satellite data sets assimilated in the CAMS data over Indian region.
4. The differences in the magnitude and sign of CC of INSAT-3DR with respect to CAMS reanalysis IPWV may be due to lack of assimilation of quality controlled data over Indian domain. This may be due to limitations of the design of the instrument /sensor on board on INSAT-3DR or retrieval algorithm of IPWV. Therefore, it will affect the overall collocations in matchup data sets.
5. The IPWV retrieved from CAMS reanalysis overestimated with respect to INSAT-3DR IPWV over land and oceanic region for all the seasons except Himalayan region and some parts of Arabian Sea and BoB. This occurred because the infrared and microwave radiometer observations of land and oceans had been assimilated into the model, which has the higher systematic humidity when it was compared with Radiosonde data (Andersson et al., 2007). Underestimation of CAMS IPWV compared with INSAT-3DR over Himalayan region may be due to presence of rugged terrain/orographic features in the retrieval of IPWV.
6. Seasonal RMSE between CAMS reanalysis and INSAT-3DR (CAMS-INSAT) retrievals are higher (>15 mm) over Bay of Bengal and pockets of Indo Gangetic Plains (IGP), North East (NE) India, Southern Parts of India, North Indian Ocean and Arabian Sea during pre-monsoon, monsoon, post monsoon season and (< 15 mm) during winter season. Higher values of RMSE prevails over the regions of higher moisture availability or water content in the Atmosphere.
7. The mean IPWV values vary in the range of 0–50 mm depending upon the region and prevailing weather system affected throughout the year. Larger mean IPWVs occur in the coastal regions of Indian Ocean regions compared to inland and desert regions due to warm air conditions as compared to inland and ocean. The south foothill of Himalayas has the largest PWV variation with a SD ~16 mm.

This study will help to improve understanding regarding representation of uncertainties associated with land, coastal and desert locations in term of seasonal flow of IPWV which is an essential integrated variable in forecasting applications.

5. Acknowledgements: Authors are grateful to Director General of Meteorology for providing data and support to accomplish this work and also thankful to the CAMS global web site data (https://ads.atmosphere.copernicus.eu) link for providing the data for the above study.

6. References.

Andersson, E., Holm, E., Bauer, P., Beljaars, S., Kelly, G. A., McNally, A.P., Simmons, A.J., Thepaut, J.n., Tompkins, A. M.: Analysis and forecast impact of the main humidity observing systems. Quaterly Journal of Royal meteorological Soc. 133:1473-1485, 2007.

Aumann, H. H., and Coauthors,: AIRS/AMSU/HSB on the Aqua mission: Design, science objectives, data products, and processing systems. IEEE Trans. Geosci. Remote Sens., 41, 253–264, 2003.

Beirle, S., Lampel, J., Wang, Y., Mies, K., Dörner, S., Grossi, M., Loyola, D., Dehn, A., Danielczok, A., Schröder, M., and Wagner, T.: The ESA GOME-Evolution “Climate” water vapor product: a homogenized time series of H2O columns from GOME, SCIAMACHY, and GOME-2, Earth Syst. Sci. Data, 10, 449-468, https://doi.org/10.5194/essd-10-449-2018, 2018.

Kaufman, Y. J., and B.-C. Gao.: Remote sensing of water vapor in the near IR from EOS/MODIS, IEEE Transactions on Geoscience and Remote Sensing, 30, 871-884, 1992.

Berrisford, p., Kallberg, P., Kobayashi, S., Dee, D., Uppala S., Simmons, A.J., Poli, P., Sato, H.: Atmospheric conservation properties in ERA-Interim. Q.J.R. Meterol. Soc. 137(659), 1381-1399, 2011.

Bevis, M., S. Businger, S. Chiswell,: GPS meteorology: Mapping zenith wet delays on to precipitable water”, J. Appl. Meteorology, 33, 379-386, 1994.

Bevis, M., S. Businger, S. Chiswell, T. A. Herring, R. A. Anthes, C. Rocken, and R. H. Ware.: GPS Meteorology: Mapping Zenith Wet Delays onto Precipitable Water.” Journal of Applied Meteorology 33 (3): 379–386. doi:10.1175/1520-0450,0332.0.CO;2,1994.

Businger, T. A. Herring, C. Rocken, R. A. Anthes, and R. H. Ware.: GPS Meteorology: Remote Sensing of Atmospheric Water Vapor Using the Global Positioning System. Journal of Geophysical Research 97 (D14): 15787. Doi: 10.1029/92JD01517, 1992.

Courcoux, N., and M. Schröder.: Vertically integrated water vapour, humidity and temperature at pressures levels and layers from ATOVS-daily means/monthly means, Satellite Application Facility on Climate Monitoring, doi:10.5676/EUM_SAF_CM/WVT_ATOVS/V001, 2013.

Emardson, T.R., Elgered, G., Johansson, J.M.: Three months of continuous monitoring of atmospheric water vapor with a network of global positioning system receivers. J Geophys Res 103(D2):1807. https://doi.org/10.1029/97JD03015, 1998.

Falaiye, O.A., Abimbola, O. J., Pinker, R.T., Perez-Ramirez, D., and Willoughby, A. A.: Multi-technique analysis of precipitable water vapor estimates in the sub-Sahel West Africa, Heliyon, 4, e00765, 2018.

Gelaro, R., McCarty, W., Suarez, M. J., Todling, R., Molod, A., Takacs, L., Randles, C. A., Darmenov, A., Bosilovich, M.G., Reichle, R., Wargan, K., Coy, L., Cullather, R., Draper, C., Akella, S., Buchard, V., Conaty, A., Da Silva, A.M., Gu, W., Kim, G.-K., Koster, R., Lucchesi, R., Merkova, D., Nielsen, J.E., Partyka, G., Pawson, S., Putman, W., Rienecker, M., Schubert, S.D., Sienkiewicz, M., Zhao, B.: The Modern-Era Retrospective Analysis for Research and applications, Version 2 (MERRA-2). J. Clim. 30, 5419–5454, 2017.

Ichoku, C., Levy, R., Kaufman, Y. J., Renner, L.A., Li, R-R., Martins, V.J., Holben, B.N., Abuhassan, N., Slutsher, I., Eck, T. F., Pietras, C.: Analysis of the performance of characteristics of the five-channel Microtops II Sun photometer for measuring the aersosl optical thickness and prexcipitable water vapouir. J. Geophys. Res. 107, 4179, 2002.

Inness, A., Ades, M., Agustí-Panareda, A., Barré, J., Benedictow, A., Blechschmidt, A.-M., Dominguez, J. J., Engelen, R., Eskes, H., Flemming, J., Huijnen, V., Jones, L., Kipling, Z., Massart, S., Parrington, M., Peuch, V.-H., Razinger, M., Remy, S., Schulz, M., and Suttie, M.: The CAMS reanalysis of atmospheric composition, Atmos. Chem. Phys., 19, 3515–3556, https://doi.org/10.5194/acp-19-3515, 2019.

Jade, S., and M. S. M. Vijayan.: GPS-Based Atmospheric Precipitable Water Vapor Estimation Using Meteorological Parameters Interpolated from NCEP Global Reanalysis Data. Journal of Geophysical Research Atmospheres 113 (3): 1–12. Doi: 10.1029/2007JD008758, 2008.

Jade, S., M. S. M. Vijayan, V. K. Gaur, T. P. Prabhu, and S. C. Sahu.: Estimates of Precipitable Water Vapour from GPS Data over the Indian Subcontinent." Journal of Atmospheric and SolarTerrestrial Physics 67 (6): 623–635. doi:10.1016/j.jastp.2004.12.010, 2005.

Jiang, J., Zhou, T., & Zhang, W.: Evaluation of satellite and reanalysis precipitable water vapor data sets against radiosonde observations in central Asia. Earth and Space Science, 6, 1129–1148. https://doi.org/10.10 29/2019EA000654, 2019.

Kishtawal, C.M.: Use of satellite observations for weather prediction, Mausam, 70, 4,709-724, 2019.

Liu, Z.; Min, M.; Li, J.; Sun, F.; Di, D.; Ai, Y.; Li, Z.; Qin, D.; Li, G.; Lin, Y.: Local Severe Storm Tracking and Warning in Pre-Convection Stage from the New Generation Geostationary Weather Satellite Measurements. Remote Sens., 11, 383, 2019.

Lee, Y. K.; Li, J.; Li, Z.; Schmit, T.: Atmospheric temporal variations in the pre-landfall environment of typhoon Nangka observed by the Himawari-8 AHI. Asia-Pac. J. Atmos. Sci. 2017, 53, 431–443, 2015.

Lee, S. J.; Ahn, M.H.; Lee, Y.: Application of an artificial neural network for a direct estimation of atmospheric instability from a next-generation imager. Adv. Atmos. Sci., 33, 221–232, 2016.

Martinez, M. A.; Velazquez, M.; Manso, M.; Mas, I.: Application of LPW and SAI SAFNWC/MSG satellite products in pre-convective environments. Atmos. Res., 83, 366–379, 2007.

Miloshevich, L. M., Vömel, H., Whiteman, D.N., and Leblanc, T.: Accuracy assessment and correction of Vaisala RS92 radiosonde water vapor measurements, Journal of Geophysical Research, 114, D11305, doi: 10.1029/2008JD011565, 2009.

Noel, S., Mieruch, S., Bovensmann, h., Burrows, J.P.: preliminary result of GOME 2 water vapour retrievals and first applecations in Polar Regions. Atmos. Chem. Phys. 8, 519-1529, 2008.

Ortiz de Galisteo, J. P., V. Cachorro, C. Toledano, B. Torres, N. Laulainen, Y. Bennouna, and A. de Frutos.: Diurnal Cycle of Precipitable Water Vapor over Spain. Quarterly Journal of the Royal Meteorological Society 137: 948–958. doi:10.1002/qj.811, 2011.

Perez Ramirez, D., Smirnov, A., Pinker, R.T., Petrenko, M., Roman, R., Chen, W., Ichoku, C., Noël, S., Gonzalez Abad, G., Lyamani, H., and Holben, B.: Precipitable water vapor over oceans from the Maritime Aerosol Network: Evaluation of global models and satellite products under clear sky conditions. Atmospheric Research, 215, 294-304, 2014.

Perez-Ramirez, D., Smirnov, A., Pinker, R.T., Petrenko, M., Roman, R., Chen, W., Ichoku, C., Noël, S., Gonzalez-Abad, G., Lyamani, H., and Holben B.N.: Precipitable water vapor over oceans from the Maritime Aerosol Network: Evaluation of global models and satellite products under clear sky conditions. Atmospheric Research, 215, 294-304. 2019.

Puviarasan, N., Yadav, Ramashray, Giri, R.K., Singh, Virendra.: GPS Meteorology: Error in the estimation of precipitable water by ground based GPS system in some meso-scale thunderstorms - A case study, Mausam, 71, 2, 175-186, 2020.

Puviarasan, N.,Sharma, A.K.,Ranalkar, Manish.,Giri, R.K.: Onset, advance and withdrawal of southwest monsoon over Indian subcontinent: A study from precipitable water measurement using ground based GPS Receivers. Journal of Atmospheric and Solar-Terrestrial Physics. 122. 10.1016/j.jastp.2014.10.010, 2014.

Ratnam, M.V, Kumar, A.H., and A. Jayaraman.: Validation of INSAT-3D sounder data with in situ measurements and other similar satellite observations over India. Atmos. Meas. Tech., 9, 5735-5745, 2016.

Saha, S.: The NCEP climate forecast system reanalysis. Bull. Am. Meteorol. Soc. 1015–1057, 2010.

Smirnov, A., B. N. Holben, A. Lyapustin, I. Slutsker, and T. F. Eck.: AERONET processing algorithms refinement, Proceedings of AERONET workshop, El Arenosillo, Spain, NASA/GSFC Aeronet project, 2004.

Smirnov, A., B. N. Holben, D. M. Giles, I. Slutsker, N. T. O'Neill, T. F. Eck, A. Macke, P. Croot, Y. Courcoux, S. M. Sakerin, T. J. Smyth, T. Zielinski, G. Zibordi, J. I. Goes, M. J. Harvey, P. K. Quinn, N. B. Nelson, V. F. Radionov, C. M. Duarte, R. Losno, J. Sciare, K. J. Voss, S. Kinne, N. R. Nalli, E. Joseph, K. Krishna Moorthy, D. S. Covert, S. K. Gulev, G. Milinevsky, P. Larouche, S. Belanger, E. Horne, M. Chin, L. A. Remer, R. A. Kahn, J. S. Reid, M. Schulz, C. L. Heald, J. Zhang, K. Lapina, R. G. Kleidman, J. Griesfeller, B. J. Gaitley, Q. Tan, and T. L. Diehl.: Maritime aerosol network as a component of AERONET- first results and comparison with global aerosol models and satellite retrievals, Atmospheric Measurement Techniques, 4, 583-597, 2011.

Susskind, J., Barnet, C.D., blaisdell, J.M.: Retrival of atmospheric and surface parameters from AIRS/AMSU/HSB data in the presense of clouds. IEE Trans. Geosci. Remote Sens. 41-390-409, 2003.

Susskind, J., Barnet, C., blaisdell, J., Iredell, L., Keita, F., Kouvaris, L., Molnar, G., Chahinnes, M.: Accuracy of geophysical parameters derived atmospheric Infrared Sounder/ Advanced Microwave Sounding Unit as a function of fraction cloud cover. J. Geophys. Res. 111, D09S17, 2006.

Trenberth, K. E.; Dai, A.; Rasmussen, R.M.; Parsons, D.B.: The changing character of precipitation. Bull. Am.Meteorol. Soc., 84, 1205–1218, 2003.

Turner, D.D., Lesht, B.M., Clough, S.A., Liljegren, J.C., Revercomb, H.E., Tobin, D.C.: Dry bias and variability in Vaisala RS80-H radiosondes: The ARM experience, Journal of Atmospheric and Oceanic Technology, 20, 117 – 132, 2003.

Viswanadham, Y.: The relationship between total precipitable water and surface dew point. J. Appl. Meteorol, 20, 3–8, 1981.

Wagner, t., Beirle, S., Grzegorski, m., Platt, U.: Global trends (1996-2003) of total coloumn precipitable water observed by Global azone monitoring Experiment (GOME) on ERS-2 and their relation to near –surface temperature. J. Geophys. Res. 111, 2006.

Yadav, Ramashray, Puviarasan, N., Giri, R.K., Tomar, C.S., Singh, Virendra.: Comparison of GNSS and INSAT-3D sounder retrieved precipitable water vapour and validation with the GPS Sonde data over Indian Subcontinent, MAUSAM, 71, 1, 551.501.86., 2020.